

Article

C8-linked pyrrolobenzodiazepine monomers with inverted building blocks show selective activity against MDR Gram-positive bacteria

Paolo Andriollo, Charlotte Hind, Pietro Picconi, Kazi S Nahar, Shirin Jamshidi, Amrit Varsha, Melanie Clifford, J Mark Sutton, and Khondaker Miraz Rahman

ACS Infect. Dis., **Just Accepted Manuscript** • DOI: 10.1021/acsinfecdis.7b00130 • Publication Date (Web): 20 Dec 2017

Downloaded from <http://pubs.acs.org> on December 21, 2017

Just Accepted

"Just Accepted" manuscripts have been peer-reviewed and accepted for publication. They are posted online prior to technical editing, formatting for publication and author proofing. The American Chemical Society provides "Just Accepted" as a free service to the research community to expedite the dissemination of scientific material as soon as possible after acceptance. "Just Accepted" manuscripts appear in full in PDF format accompanied by an HTML abstract. "Just Accepted" manuscripts have been fully peer reviewed, but should not be considered the official version of record. They are accessible to all readers and citable by the Digital Object Identifier (DOI®). "Just Accepted" is an optional service offered to authors. Therefore, the "Just Accepted" Web site may not include all articles that will be published in the journal. After a manuscript is technically edited and formatted, it will be removed from the "Just Accepted" Web site and published as an ASAP article. Note that technical editing may introduce minor changes to the manuscript text and/or graphics which could affect content, and all legal disclaimers and ethical guidelines that apply to the journal pertain. ACS cannot be held responsible for errors or consequences arising from the use of information contained in these "Just Accepted" manuscripts.



C8-linked pyrrolobenzodiazepine monomers with inverted building blocks
show selective activity against MDR Gram-positive bacteria

Paolo Andriollo¹⊥, Charlotte K. Hind²⊥, Pietro Picconi¹, Kazi S Nahar¹, Shirin Jamshidi¹, Amrit Varsha¹, Melanie Clifford², J. Mark Sutton^{2*} and Khondaker Miraz Rahman^{1*}.

¹Institute of Pharmaceutical Science, King’s College London, 150 Stamford Street, London SE1 9NH, UK.

²Public Health England, National Infections Service, Manor Farm Road, Porton Down, Salisbury SP4 0JG, UK.

⊥ These authors contributed equally to the manuscript.

Corresponding authors

For KMR: e-mail k.miraz.rahman@kcl.ac.uk

For JMS: e-mail mark.sutton@phe.gov.uk

Antimicrobial resistance has become a major global concern. Development of novel antimicrobial agents for the treatment of infections caused by multidrug-resistant (MDR) pathogens is an urgent priority. Pyrrolobenzodiazepines (PBDs) are a promising class of antibacterial agents initially discovered and isolated from natural sources. Recently C8-linked PBD biaryl conjugates have been shown to be active against some MDR Gram-positive strains. To explore the role of building block orientations on antibacterial activity and obtain SAR information, four novel structures were synthesized in which the building blocks of previously reported compounds were inverted, and their antibacterial activity studied. The compounds showed MICs in the range of 0.125 $\mu\text{g/mL}$ to 32 $\mu\text{g/mL}$ against MDR Gram-positive strains with a bactericidal mode of action. The results showed that a single inversion of amide bonds reduces the activity while the double inversion restores the activity against MDR pathogens. All inverted compounds did not stabilize DNA and lacked eukaryotic toxicity. The compounds inhibit DNA gyrase *in vitro*, and the most potent compound was equally active against both wild-type and mutant DNA gyrase in a biochemical assay. The observed activity of the compounds against MRSA strains with equivalent gyrase mutations is consistent with gyrase inhibition being the mechanism of action *in vivo*, although this has not been definitively confirmed in whole cells. This conclusion is supported by a molecular modelling study showing interaction of the compounds with wild-type and mutant gyrases. This study provides important SAR information about this new class of antibacterial agents.

KEYWORDS

Antimicrobial Resistance, Medicinal Chemistry Optimization, Minimum Inhibitory Concentration, Pyrrolobenzodiazepine, ESKAPE Pathogens

The resistance of pathogens to antibacterial agents has become a major global concern. Multiple drug resistant (MDR) bacteria cause many common and severe infections for which treatment is increasingly becoming difficult or in some cases impossible.¹ The spread of healthcare-associated infections and associated antimicrobial resistance is facilitated by interspecies gene transmission, poor sanitation, and hygienic conditions, along with the increasing frequency of global travel, trade and disease transmission.² Of great concern among all the bacteria that are developing resistance, is a group of pathogens termed the ESKAPE pathogens,³ which are characterized by the rapid acquisition of resistance to multiple classes of antibiotic (with resistance to 3 or more classes referred to as multidrug resistance). These species are primarily associated with nosocomial infections especially amongst immunocompromised patients⁴ and this also has an additional economic impact upon the healthcare system.^{1, 5} Although the measurement of additional costs is complicated⁶ the estimated economic impact for the U.S. economy is reported to be higher than \$20 billion in direct annual healthcare costs.⁷

In the last 30 years, no major classes of broad spectrum antibiotics have been introduced to the market and recently approved agents like linezolid (2000), daptomycin (2003), and retapamutilin (2007) are active only against Gram-positive pathogens.⁸ A recent report from the World Health Organisation has highlighted the limited number of drugs in the pipeline with only a few molecules in phase 2 and 3 of clinical development against ESKAPE pathogens; these are predominantly focused on Gram-positive species or are iterations of existing drugs (notably beta-lactamase inhibitor combinations). This highlights the need to identify and evaluate new therapeutic options and/or to modify existing chemical scaffolds to obtain antibiotics with

improved properties¹⁰ and a number of agents developed through this approach are currently undergoing clinical trials.⁹

Applying the same principle, we selected the pyrrolobenzodiazepines (PBDs) as a relatively unexplored chemical scaffold to generate new antibacterial compounds with improved bioactivity, and elucidate the structure activity relationship (SAR) of C8-linked PBDs. PBDs are naturally occurring molecules produced by *Streptomyces* bacteria whose family members include anthramycin and tomaymycin.^{11, 12} PBDs are a class of sequence-specific DNA minor groove binding agents that are selective for GC-rich sequences, which have been evaluated as potential chemotherapeutic agents in recent years.¹³ PBDs have a chiral centre at their C11a(*S*)-position which provides an appropriate 3D shape for them to fit securely within the DNA minor-groove. They also possess a “soft” electrophilic imine moiety at their N10-C11 position which can form an aminor linkage between their C11-position and the C2-NH₂ group of a guanine base only when the molecule is secure within the minor groove.^{14, 15} Anthramycin was the first naturally derived PBD, initially discovered and isolated in 1963 from *Streptomyces* and *Micrococci* bacteria¹⁶, and later many other natural and synthetic PBDs followed. Naturally occurring PBDs such as anthramycin, tomaymycin, neothramycin and sibiromycin form adducts that span three base pairs, with guanine in the central position,^{17, 18} and their preferred binding site is 5'-AGA-3',¹⁹ although more recent data suggest that they have a kinetic preference for 5'-Py-G-Py-3' sequences.²⁰ PBD monomers can recognize and bind to specific sequences of DNA and therefore have the potential to act as competitive inhibitors of transcription factors. Considering their mechanism of action, PBDs have been extensively studied as anticancer agents but relatively unexplored as antibacterial agents.²¹⁻²⁴ Different studies showed the possibility of synthesizing

PBD analogues characterized by their high selectivity for particular DNA sequences, by modifying the C8 position substituent.^{25, 26} For example, PBD-biaryl conjugates, a subclass of monomers with C8-subunits, have shown preferences for GC sequences.²⁷ Molecules belonging to this subclass have been demonstrated to be well tolerated in mice at high concentrations, and molecular dynamics simulations indicate that they are easily accommodated within the minor groove causing little distortion to DNA structure.

We previously studied numerous PBD-biaryl conjugated structures, and identified some characteristics that are important for optimal antibacterial activity against Gram-positive pathogens.²⁴ Among the compounds studied, we selected two compounds which showed excellent antibacterial activity against MDR Gram-positive pathogens (MIC range: 0.003-0.125 $\mu\text{g/mL}$) for our investigation. The first compound is a PBD-Py-Bzf (Py = pyrrole, Bzf = benzofuran) conjugate, while the second structure was PBD-Py-Bzt (Bzt = benzothiophene) (**Figure 1**) conjugate. Starting from these two molecules we designed four new molecules with a different orientation of the building blocks constituting the C8 lateral chain. It has been reported in the literature that the standard orientation of the amide bonds provide additional hydrogen bond contact with the minor groove of DNA, and inversion of the amide linkage should result in loss of these contacts and reduced binding to DNA.^{23, 25} There is a positive correlation between DNA binding and eukaryotic toxicity of PBD monomers and a reduction in binding should result in reduction or loss of toxicity. Firstly, we wanted to investigate the antibacterial activity of the derivatives characterized by the inversion of the amide linkage between *N*-methylpyrrole and the alkyl spacer and later the derivatives with both the reverse *N*-methylpyrrole and the amide bonds between the building blocks (**Figure 2**), and obtain

1
2
3 compounds with reduced eukaryotic toxicity. To achieve the synthesis of these new PBD-C8-
4 benzofused conjugates we needed a new PBD core with a 4C-NH₂ linker in place of traditional
5 4C-COOH linker. Tiberghien *et al.* reported the use of this functionality in 2008²⁸ for the
6 synthesis of PBD dimers, but in this work, for the first time, it was used for the synthesis of C8-
7 linked PBD monomers and the synthesized compounds are the first examples of C8-linked PBD
8 monomers with an inverted amide linkage between the 4C-spacer and the heterocyclic building
9 blocks. Moreover, from a synthetic chemistry point of view, this modification allowed us to
10 avoid the protection of the hydroxyl group at C11, otherwise necessary to prevent the
11 racemization of (*S*) C11a observed in the previous synthesis during the basic methyl ester
12 hydrolysis employed in C8-PBD monomer synthesis²³
13
14
15
16
17
18
19
20
21
22
23
24
25
26
27

28 The newly synthesized compounds were tested against susceptible and MDR Gram-positive
29 bacterial strains. The compounds were also tested in a FRET based DNA melting assay, to
30 evaluate the effect of inverse orientation on the DNA binding ability of the compounds, and
31 against mammalian cell lines to assess their selectivity for prokaryotic cells. The mechanism of
32 action of the compounds were studied initially by an *in silico* screening against bacterial targets,
33 followed by a biochemical assay against the wild-type and mutant target identified by the *in*
34 *silico* study. Finally, molecular modelling experiments were performed to rationalize the
35 obtained biological results.
36
37
38
39
40
41
42
43
44
45
46
47
48
49
50
51
52
53
54
55
56
57
58
59
60

RESULT AND DISCUSSION

Chemistry. Both the synthetic strategies followed for the synthesis of the core bearing the 4C-COOH (**Scheme 1**) and the core bearing 4C-NH₂ functionality are based on the previously reported Thurston/Rahman approach.²³ The PBD core used to synthesize the final compounds with standard orientation was obtained as Alloc-THP-protected PBD unit (**9**). Briefly, vanillin was alkylated with methyl 4-bromobutyrate employing K₂CO₃ in DMF providing the ester derivative **1** after precipitation. Subsequently, **1** underwent a selective nitration reaction using KNO₃/TFA to give **2** in good yield after an aqueous work-up. The nitrobenzaldehyde derivative **2** was then oxidized to the carboxylic acid intermediate **3** using KMnO₄. The key intermediate **4** was obtained by amide coupling between **3**, which had been activated to the corresponding acid chloride by treatment with oxalyl chloride, and optically pure (*S*)-pyrrolidine methanol. Reduction of the nitro derivative **4** to the corresponding amino derivative **5** was accomplished with Pd/C in a Parr hydrogenator system at 40 psi, followed by Alloc protection gave **6** in good yield after purification by column chromatography. The Alloc-protected PBD ring system **7** was then obtained by oxidative cyclization using the BAIB/TEMPO oxidizing system. In order to prevent racemization at the C11a position of the PBD ring system, which occurs under alkaline conditions, the alcohol derivative **7** was protected with a THP ether giving **8**. The final Alloc-THP-protected PBD capping unit **9** was obtained via hydrolysis of the methyl ester using 0.5 M NaOH aqueous solution.

The synthetic strategy to obtain the C8-linked PBDs with inverted amide bonds (**Scheme 2**) involved protection of the reactive amino group on the 4C-spacer to avoid side reactions, and the reaction steps were adjusted taking this modification into account. Particularly, acidic conditions

were avoided after the introduction of the Boc-protected amine side chain. To obtain the type 2 core, vanillin was coupled with benzyl bromide under alkaline condition giving the ether derivative **10** after recrystallization. This additional step allowed the selective nitration that led to **11** with a good yield. The benzyl group was then removed with concentrated HBr in acetic acid to afford the nitro-vanillin derivate **12**. The amide coupling reaction with (*S*)-pyrrolidine methanol to obtain **15** was performed using HBTU and DIPEA rather than oxalyl chloride to avoid the generation of acid. The final Alloc-protected PBD capping unit was obtained via the de-protection of the amino group by TFA in DCM, just before the coupling with the selected tail.

The synthesis of the C8-side chains was achieved by amide coupling between the selected building blocks (**Scheme 3**). An EDCI/DMAP reagents system was used for the activation of the acid, leading to intermediate **19** to **24** with variable yield (20% to 93%). Nitrile groups of **20** and **23** were hydrolyzed by refluxing in dioxane in a strongly acidic environment (with the presence of H₂SO₄) to give **25** and **26** after purification by column chromatography.

The last step in the synthesis of the C8-linked benzofused-*N*-methylpyrrole PBD derivatives consisted of several sequential passages. At first, when it was necessary, the capping units were de-protected. Methyl esters of derivatives **21** and **24** were hydrolyzed under basic conditions (in a NaOH aqueous solution), leading to the acid compounds, while the amino groups on **19** and **22** were de-protected in an acidic environment (TFA in DCM). Subsequently, the PBD core and the benzofused-*N*-methylpyrrole tails were connected through an amide coupling reaction. Once again, EDCI/DMAP system was used to carry out acid activation and coupling. Finally, the conjugated products were de-protected with pyrrolidine and Pd(PPh₃)₄ in DCM, affording the

final compounds **27**, **28**, **29**, **30**, **31** and **32** (Scheme 4). The final de-protection was common to all the products regardless of the presence of THP protection, and both the protected and the final PBD imine conjugates were purified by column chromatography.

Evaluation of DNA binding ability of the synthesized compounds

The ability of compounds **27**, **28**, **29**, **30**, **31** and **32** to bind and stabilize the DNA was evaluated using a FRET-based DNA melting assay²⁹ to understand the effect of building block orientation on the DNA binding ability of the compounds. The compounds were tested using two fluorophore-labelled oligonucleotide sequences (Sequence F1: 5'-FAM-TAT-ATA-TAG-ATA-TTT-TTT-TAT-CTA-TAT-ATA-3'-TAMRA, and Sequence-F2: 5'-FAM-TAT-AGA-TAT-AGA-TAT-TTT-ATA-TCT-ATA-TCT-ATA-3'-TAMRA). Netropsin, a known DNA minor groove binder, was used as a positive control. The result of the assay is reported in **Table 1**. Previously reported C8-PBD conjugates **27** and **30**, and control compound netropsin showed notable stabilization of both DNA sequences at 1 μ M, but the C8-PBD compounds with inverted building blocks, **28**, **29**, **31** and **32** did not stabilize the DNA sequence, with ΔT_m values < 1 °C at 1 μ M concentration (drug:DNA ratio 5:1). The result suggests the inversion of single or both amide bonds reduced the ability of these compounds to interact with and stabilize the DNA sequences.

Evaluation of Eukaryotic Toxicity

The inability of the inverted C8-PBD conjugates to stabilize DNA sequences suggested the compounds may show reduced toxicity against eukaryotic cell lines, as DNA stabilization has been associated with cytotoxicity for PBD-type covalent minor groove binders.³⁰ The eukaryotic cytotoxicity of the synthesized compounds was tested against the cervical cancer cell line HeLa

1
2
3 and the non-tumor lung fibroblast WI38 using an MTT assay.³¹ The original C8-PBD
4 benzofused conjugates **27** and **30** showed very potent cytotoxicity against the HeLa cell line
5
6 (**Figure 3**) with only 25% and 32% cells viable after 24 hours. The compounds showed slightly
7
8 less toxicity against the non-tumor cell line WI 38 with 42% and 47% cells viable after 24 hours.
9
10 However, the inverted compounds **28**, **29**, **31** and **32** showed notably less toxicity against both
11
12 HeLa and WI38 cell lines. In the case of the inverted compounds >70% of cells were viable after
13
14 24 hours treatment with the molecules. This lack of toxicity was in line with the DNA binding
15
16 ability of the compounds, and this is consistent with previous reports that PBDs exert their
17
18 cytotoxicity by alkylating and stabilizing DNA sequences.³²
19
20
21
22
23
24
25
26
27
28
29
30
31
32
33
34
35
36
37
38
39
40
41
42
43
44
45
46
47
48
49
50
51
52
53
54
55
56
57
58
59
60

Microbiological Evaluation

The inverted amide compounds and the parent compounds were tested against a selected panel of Gram-positive bacteria to assess their antibacterial activity (**Table 2**). The Gram-positive panel was comprised of *Staphylococcus aureus* and *Enterococcus spp.* strains, which comprise the ‘S’ and the ‘E’ from the ESKAPE pathogens acronym. The strains used were; methicillin sensitive *S. aureus* (MSSA) strain ATCC 9144, two methicillin resistant *S. aureus* (MRSA) strains, EMRSA-15 (strain HO 5096 0412) and EMRSA-16 (strain MRSA 252), vancomycin sensitive *E. faecalis* (VSE), strain NCTC 755, vancomycin resistant *E. faecalis* (VRE), strain NCTC 12201 and vancomycin resistant *E. faecium* (VRE), strain NCTC 12204. As expected, compound **27** showed good antibacterial activity with MICs lower than 0.125 µg/mL against all Gram-positive strains tested. Surprisingly, the inversion of one amide linkage in compound **28** resulted in a considerable loss of activity with an MIC of 2 µg/mL against VRE strains and 16 µg/mL against VSE and MSSA strains. The drop in activity was particularly surprising against MRSA strains, with an MIC higher than 32 µg/mL. Interestingly, compound **29**, characterized by the inversion of both the amide linkages and of the *N*-methylpyrrole building block, presented a better antibacterial profile than **28**. Although it was found to be less potent than **27**, compound **29** maintained moderate activity against the bacterial strains with MICs in the range between 0.5 and 4 µg/mL. The observations made for the benzofuran series of C8-PBD conjugates were further confirmed by evaluating the C8-benzothiophene series of inverted and parent PBD compounds (**Table 2**). Compound **32** showed antibacterial activity comparable to previously reported compound **30** against *Enterococci* strains with MICs lower than 0.125 µg/mL. However, a drop in activity was observed against *S. aureus* strains with MICs higher than 32 µg/mL against MRSA and of 16 µg/mL against MSSA. Compound **31** showed antibacterial activity similar to **32** against *S. aureus* strains, but generally showed higher MICs

1
2
3 against other strains. Overall, the inverted C8-linked benzothiophene PBD compounds showed
4
5 better antibacterial activity against *Enterococcus* strains compared to the benzofuran compounds,
6
7 while among the four newly synthesized compounds, the inverted benzofuran derivative **29** was
8
9 found to be most active against *S. aureus* strains.
10
11
12

13
14 The mode of action of compound **29** was explored using time-kill assays. One MRSA (EMRSA-
15
16 15) and one VRE (NCTC 12201) strain were treated with compound **29** at 4 × MIC for 24 hours
17
18 and cell counts elucidated at specified time points. The results show a rapidly bactericidal mode
19
20 of action in both strains for compound **29**, with cell counts falling below the limit of detection
21
22 within 2 hours, whilst the control antibiotic ciprofloxacin displayed a bacteriostatic mode of
23
24 action (**Figure 4**). Although a small population of cells was detected after 24 hours of treatment
25
26 with compound **29** in EMRSA-15 (in two of three replicate experiments), no resistance to the
27
28 compound was detected in this population (assessed by determining the MIC of surviving cells),
29
30 and as such they most likely represent a persister population. This is observed in EMRSA15
31
32 (fluoroquinolone resistant) but not in strain NCTC12201 (fluoroquinolone sensitive), although
33
34 the role of fluoroquinolone resistance in persister survival in these assays is unproven.
35
36
37
38
39
40
41

42 ***In silico* DNA Interaction Study:** In order to rationalize the obtained results, a molecular
43
44 modelling study was carried out using three random sequences of DNA. AT-rich Seq-1 (5'-
45
46 TATATAAGATATATATA- 3'), GC-rich Seq-2 (5'-TAGCTAGCTAGCTAGCG-3') and mixed
47
48 AT/GC Seq-3 (5'-GCGCGCGCGCGGCGCGC-3'). Covalent molecular docking between the N
49
50 atom of NH₂ group of Guanine and the C11 atom of C=N imine bond in PBDs, showed
51
52 favorable complexes with good affinities between PBDs and DNA. As PBDs are known to work
53
54
55
56
57
58
59
60

by interacting with the DNA minor groove, we calculated the relative binding free energy of the DNA-compound complex (**Figure 5**) using molecular dynamics simulations followed by Molecular Mechanics-Poisson Boltzmann Surface Area (MM-PBSA) / Molecular Mechanics-Generalized Born Surface Area (MM-GBSA) calculations (**Table 3**). These models showed favorable energy values of ΔG_{GB} and ΔG_{PB} for the reference compounds in all three sequences while the results for the inverted compounds (**28**, **29**, **31** and **32**) were considerably lower than the parent compounds **27** and **30**. The modelling study supported the lack of DNA stabilization observed in the FRET melting study and the lack of eukaryotic toxicity. Overall, a positive correlation between the free energy of binding and antibacterial activity was observed suggesting DNA binding plays a role in the antibacterial potency of these compounds.

Mechanistic Evaluation

As the inverted C8-analogues did not stabilise DNA sequences and were non-toxic to eukaryotic cells, the mechanism of action of these molecules is likely to be DNA independent. To explore this further, we carried out an *in silico* docking campaign with known bacterial targets (ESI) to get an indication of the mechanism of action of these inverted pyrrolobenzodiazepines. Among the targets studied, the inverted compound **29** interacted with the ligand binding domain of DNA gyrase and showed excellent affinity towards both sub-units of bacterial DNA gyrase. The best pose of compound **29** with the bacterial gyrase from *Staphylococcus aureus* (PDB ID 2XCT) which gave a CHEM Score of 21.68 and affinity of -29 (kcal/mol) for subunit 1 of Gyrase A, and a CHEM Score of 23.29 and affinity of -30 (kcal/mol) for subunit 2 of Gyrase A (**Figure 6** and **Table S2**). The 2D models shown in Figure 6C suggests compound **29** forms three conventional hydrogen bonds with serine 98, arginine 92 and glutamine 95 of the subunit 1 of DNA gyrase A. Other key interactions are reported in Table S4. Similarly, compound **29** also forms three

conventional hydrogen bonds with serine 85, arginine 92 and serine 98 of the subunit 2 of Gyrase A (**Figure 6D**). A number of hydrophobic and electrostatic interactions with different amino acids from subunits of Gyrase A were also observed (**Table S5**). The interaction of **29** with the ligand binding site of Gyrase A suggests the antimicrobial activity is due to the inhibition of Gyrase A by directly interacting with the enzyme, and not due to its ability to associate with DNA.

The *in silico* observation was validated by carrying out a DNA gyrase inhibition assay using a commercial *S. aureus* gyrase supercoiling high throughput plate assay (#SATRG01) kit obtained from Inspiralis (Norwich, UK) (**Figure 7 and S4**). Compound **29** inhibited wild-type gyrase isolated from *S. aureus* with an IC_{50} of 0.95 ± 0.30 $\mu\text{g/mL}$ which is significantly ($P < 0.05$) better than ciprofloxacin which inhibited the wild-type gyrase with an IC_{50} of 2.85 ± 1.80 $\mu\text{g/mL}$. Surprisingly, compound **27** and **30** also showed comparable IC_{50} s, 1.65 ± 0.68 $\mu\text{g/mL}$ and 2.28 ± 0.98 $\mu\text{g/mL}$, respectively, against wild type gyrase (**Figure 7**). There was no statistically significant difference between the IC_{50} of compounds **27**, **29** and **30**. This data does not provide a clear differential in gyrase inhibition between compounds that stabilise DNA (**27** and **30**) and may inhibit gyrase, a DNA associated enzyme, and compounds that have not shown DNA stabilisation (**29** and ciprofloxacin, **Table 1**), where we would infer direct inhibition by gyrase binding. Competition assays were used to try and define the basis of the interaction. However, no clear answer could be obtained, as doubling the concentration of enzyme in the gyrase assays reduced the inhibition caused by compound **29** and ciprofloxacin but not compound **30**, which supports our inference, but a reduction in inhibition was also observed for compounds **27** which could not be explained (**Figure S5**).

One of the most common mutations found in fluoroquinolone resistant *S. aureus* strains is the S84L mutation in the gyrA subunit. We tested compound **29** against a gyrase enzyme complex containing this mutation and found that at 20 µg/ml, compound **29** inhibited the mutant enzyme by 60.0% ±11.2%, whilst ciprofloxacin inhibited the mutant enzyme by just 43.3% ±1.1 at the higher concentration of 32 µg/ml (**Figure S9**). This data suggests that compound **29** retains better activity against the fluoroquinolone-resistant enzyme than ciprofloxacin. The ability of compound **29** to inhibit the mutated DNA gyrase led us to carry out a further molecular modelling study to rationalize the biochemical assay result. The molecular model of gyrase A with S84L mutation in the gyrA subunit was developed with PyMol using PDB ID 2XCT as the template. The structure was minimized, equilibrated and subsequently validated by AMBER package program. Interestingly, compound **29** interacted with the ligand binding site of mutant Gyrase A (**Figure S2**) with greater affinity and higher CHEMSCORE (23.4 for subunit 1 and 23.4 for subunit 2) compared to the wild-type enzyme. However, ciprofloxacin showed a significantly reduced affinity and CHEMSCORE (15.8 for subunit 1 and 15.9 for subunit 2) for the mutant enzyme (**Figure S3, Table S3**), which is consistent with the literature. Compound **29** formed five conventional hydrogen bonds with both subunit 1 and subunit 2 of the mutant enzyme (**Tables S6 and S7**). The antibacterial activity observed for compound **29** against *Staphylococcus* strains (**Table 2**) appeared to support the biochemical assay and the *in silico* observation as it showed similar activity (MIC 2-4 µg/mL) against the MSSA strain ATCC9144, which doesn't bear the S84L mutation in gyrase A and the MRSA strains, EMRSA-15 and EMRSA-16, with the S84L mutation in gyrase A.

Conclusions. This study was focused on understanding how the building blocks orientation of the lateral C8 side chain of PBDs affect the antibacterial activity of C8-PBD conjugates, and the suitability of developing C8-linked inverted PBDs as antibacterial agents. Furthermore, we explored the suitability of using the novel 4C-NH₂ linker on the C8-position of the PBDs, which provides some advantages for the synthesis of the C8-linked pyrrolobenzodiazepines by avoiding the base catalyzed hydrolysis step that can result in C11a racemization. Four inverted C8-linked benzofused PBDs were successfully synthesized employing both 4C-COOH and 4C-NH₂ linkers. Two of them presented the inversion of the amide linkage between *N*-methylpyrrole and the PBD core while the other two presented the inversion of both amide bonds between the three moieties constituting the lateral chain and the heterocyclic building blocks. The single amide bond inverted compounds showed notably inferior antibacterial activity owing to their inability to effectively associate with the DNA minor groove. However, the double inverted compounds showed comparable activity to the C8-benzofused PBDs with natural orientation. The inverted C8-analogues did not stabilize DNA sequences and showed selective toxicity towards prokaryotic cells. The differential sensitivity observed between *S. aureus* and *Enterococcus spp.* for compounds **31**, **32** and, to a lesser extent, **28**, is intriguing and pointed towards a new mechanism of action rather than solely DNA-binding, as observed for traditional DNA minor groove binders. *In silico* studies followed by biochemical assays suggested that the compounds are capable of binding to DNA gyrase and showed inhibition of DNA gyrase in vitro. . The data in this study shows that these molecules can inhibit both wild-type and mutant DNA gyrase (S84L mutation in gyrase A) enzymes in vitro and kill *S. aureus* strains, carrying this mutation, that are resistant to fluoroquinolones. The observed IC₅₀ is comparable to ciprofloxacin in the in vitro assay, and this was also the case for non-inverted PBDs (**27** and **30**). Future studies are

1
2
3
4
5
6
7
8
9
10
11
12
13
14
15
16
17
18
19
20
21
22
23
24
25
26
27
28
29
30
31
32
33
34
35
36
37
38
39
40
41
42
43
44
45
46
47
48
49
50
51
52
53
54
55
56
57
58
59
60

required to re-evaluate of the mechanism of bacterial killing by this class of molecules, both in terms of the kinetics of the in vitro gyrase inhibition assay and by showing bacterial responses which are consistent with DNA-gyrase inhibition *in vivo*. This deeper understanding of the mechanism of action provides an opportunity to develop these inverted C8-PBD analogues as antibacterial agents due to their lack of eukaryotic toxicity and reasonable activity against MDR Gram-positive pathogens, potentially reviving PBD based anti-infective research.

METHODS

Chemistry. All solvents and reagents for the synthesis were obtained from commercially available sources, including, among others, Sigma-Aldrich, Fisher Scientific, Fluorochem and Alfa Aesar. Thin-layer-chromatography (TLC) analysis was performed on silica gel plates (E. Merck silica gel 60 F254 plates) and visualized by ultra-violet (UV) radiation at 254 nm. Flash chromatography for the purification of compound was performed with silica gel as a stationary phase (Merck 60, 230-400 mesh). ^1H and ^{13}C nuclear magnetic resonance (NMR) analyses were performed on a Bruker Spectrosp in 400Hz spectrometer. IR spectra were collected with an FT/IR IRAffinity-1S IR spectrophotometer (Shimadzu). HRMS was performed on a Thermo Scientific-Exactive HCD Orbitrap Mass Spectrometer. LC-MS analyses were performed on a Waters Alliance 2695 system, eluting in gradient with a flow rate of 0.5 mL/min using a solvent gradient starting with 5% acetonitrile that was increased to 95% acetonitrile over a 7.5 minutes' time period (ESI). The analyses were performed on a Monolithic C18 50×4.60 mm column (made by Phenomenex). UV detection was performed on a Diode Array Detector. Mass spectra were registered in both the ESI+ and ESI- mode. The hydrogenation reaction was conducted using a Parr hydrogenation system. Dynamic light scattering experiment was performed using a Nanoseries machine (Malvern Instruments, UK).

Methyl 4-(4-formyl-2-methoxyphenoxy)butanoate (1). Methyl 4-bromobutanoate (17.7 mL, 140.2 mmol, 1.05 equiv.) and potassium carbonate (30.4 g, 210.3 mmol 1.5 equiv.) were added to a solution of vanillin (20.0 g, 131.4 mmol, 0.9 equiv.) in DMF (80 mL). The suspension was stirred at room temperature for 6 h, until TLC showed the completion of the reaction. At that point H_2O (1 L) was added to the reaction, causing the formation of a precipitate that was filtered and collected giving pure **1** (32.0 g, 95%) as a white solid (m.p. 65 °C).

R_f value (100% DCM): 0.62; ^1H NMR (400 MHz, CDCl_3) δ 9.84 (1H, s), 7.40-7.44 (2H, m), 6.98 (1H, d, $J = 8$ Hz), 4.16 (2H, t, $J = 6.2$ Hz), 3.92 (3H, s), 3.69 (3H, s), 2.56 (2H, t, $J = 7.2$ Hz), 2.17-2.23 (2H, m). ^{13}C NMR (100 MHz, CDCl_3) δ 190.9, 173.4, 153.8, 149.9, 130.3, 126.8, 111.5, 109.2, 67.8, 56.4, 51.7, 30.3, 24.2. m/z (+ESI) calc. for $\text{C}_{13}\text{H}_{16}\text{O}_5$ (M) $^+$ 252.2 found 253.1 ($[\text{M}+\text{H}]^+$).

Methyl 4-(4-formyl-2-methoxy-5-nitrophenoxy)butanoate (2). A solution of **1** (10.0 g, 39.6 mmol, 1.0 equiv.) in trifluoroacetic acid (12 mL) was added dropwise to a solution of KNO_3 (5.0 g, 49.5 mmol, 1.25 equiv.) in trifluoroacetic acid (12 mL) kept at 0°C under a magnetic stirrer. After 40 min, TLC and LCMS monitoring showed completion of the reaction. The reaction mixture was evaporated under reduced pressure using a rotary evaporator. The residue was dissolved in EtOAc (50 mL), and the organic phase was washed with brine (3×50 mL). The organic phases were dried over MgSO_4 and concentrated by a rotary evaporator giving pure **2** (10.7 g, 92%) as an amber oil.

R_f value (100% DCM): 0.72; ^1H NMR (400 MHz, CDCl_3) δ 10.29 (1H, s), 7.46 (1H, s), 7.11 (1H, s), 4.06 (2H, t, $J = 6.2$ Hz), 3.85 (3H, s), 3.56 (3H, s), 2.42 (2H, t, $J = 7.2$ Hz), 2.04-2.11 (2H, m); ^{13}C NMR (100 MHz, CDCl_3) δ 188.5, 172.8, 152.7, 150.9, 143.5, 124.7, 110.5, 108.2, 67.8, 56.4, 51.3, 29.7, 23.2 m/z (+ESI) calc. for $\text{C}_{13}\text{H}_{15}\text{NO}_7$ (M) $^+$ 297.2 found 298.1 ($[\text{M}+\text{H}]^+$).

5-Methoxy-4-(4-methoxy-4-oxobutoxy)-2-nitrobenzoic acid (3). Compound **2** (10.0 g, 33.6 mmol, 1.0 equiv.) was dissolved in acetone (400 mL). A hot solution of 10% potassium permanganate (275 mL) was added to the solution of **2** in a flask fitted with a condenser. The reaction mixture was left under reflux until the reaction went to completion (according to TLC). At that point, the reaction mixture was cooled down to room temperature. The brown residue formed was filtered through a celite patch and washed with 600 mL hot H₂O. A solution of 16% sodium bisulphite in 1N HCl (400 mL) was added to the filtrate, and the pH of the solution was adjusted to 1 using concentrated HCl. This caused the precipitation of a yellow solid that was filtered, collected and dried giving pure **3** (9.0 g, 82%) as a yellow solid (m.p. 114 °C).

R_f value (EtOAc:MeOH 50:50): 0.4; ¹H NMR (400 MHz, CDCl₃) δ 7.38 (1H, s), 7.21 (1H, s), 4.15 (2H, t, *J* = 5.8 Hz), 3.97 (3H, s), 3.70 (3H, s), 2.56 (2H, t, *J* = 7.2 Hz), 2.17-2.24 (2H, m); ¹³C NMR (100 MHz, CDCl₃) δ 172.8, 166.0, 151.8, 149.1, 141.2, 121.3, 111.5, 107.2, 68.3, 56.4, 51.3, 29.7, 23.8. *m/z* (+ESI) calc. for C₁₃H₁₅NO₈ (M)⁺ 313.2 found 312.1 ([M]-H)⁻

(S)-Methyl 4-(4-(2-(hydroxymethyl)pyrrolidine-1-carbonyl)-2-methoxy-5-nitrophenoxy)butanoate (4). A solution was prepared by dissolving **3** (7.9 g, 25.2 mmol, 1.0 equiv.) in dry DCM (50 mL) in a round bottom flask previously dried in an oven. Oxalyl chloride (6.5 mL, 75.6 mmol, 3 equiv.) and a catalytic amount of DMF (2-3 drops) were added to the solution that initiated the reaction. The solution was left under a magnetic stirrer for 1 h until it ceased the formation of HCl. Dry toluene (15 mL) was added to the reaction mixture that was evaporated under reduced pressure in a rotary evaporator to eliminate the excess of oxalyl chloride. The reaction mixture was dissolved in dry DCM (50 mL) and the solution was dropwise added to a solution of triethylamine (10.5 mL, 75.6 mmol, 3 equiv.) and +(S)-

pyrrolidinemethanol (3.7 mL, 37.8 mmol, 1.5 equiv.) in dry DCM (30 mL) kept at 0 °C under N₂ atmosphere. The reaction mixture was then allowed to stir overnight. After 15 h TLC showed the completion of the reaction, and the reaction mixture was extracted using 1 N HCl (2×70 mL) and brine (2×70 mL). The combined organic fractions were dried over MgSO₄ and concentrated by the rotary evaporator to give a yellow oil. The crude was purified by column chromatography (mobile phase: from EtOAc, 100, v/v to EtOAc /MeOH, 98/2, v/v) affording pure **4** (5.5 g, 55%) as a pale yellow solid (m. p. 82 °C).

R_f value (EtOAc:MeOH 90:10): 0.46; ¹H NMR (400 MHz, CDCl₃) δ 7.69 (1H, s), 6.79 (1H, s), 4.14 (2H, t, *J* = 4.4 Hz), 3.96 (3H, s), 3.90 (1H, m), 3.78 (1H, m), 3.69 (3H, s), 3.16 (2H, t, *J* = 6.8 Hz), 2.55 (2H, t, *J* = 4.8 Hz), 2.10-2.22 (3 H, m), 1.70-1.90 (4 H, m); ¹³C NMR (100 MHz, CDCl₃) δ 173.2, 154.8, 148.4, 109.2, 108.4, 68.4, 66.1, 61.5, 56.7, 51.7, 49.5, 30.3, 28.4, 24.4, 24.2. m/z (+ESI) calc. for C₁₈H₂₄N₂O₈ (M)⁺ 396.3 found 397.0 ([M]+H)⁺.

(S)-Methyl 4-(5-amino-4-(2-(hydroxymethyl)pyrrolidine-1-carbonyl)-2-

methoxyphenoxy)butanoate (5). A catalytic amount of Pd/C (10% w/w) was added to a solution of **4** (5.5 g, 13 mmol, 1 equiv.) in EtOH (100 mL). The reaction mixture was hydrogenated in a Parr hydrogenator at 40 psi until for 4 h when TLC showed the completion of the reaction. At that point, the reaction was filtered under vacuum through a patch of celite. The resulting solution was evaporated using rotary evaporator giving pure **5** (4.5 g, 95 %) as a dark yellow solid (m. p. 46 °C).

R_f value (EtOAc:MeOH 90:10): 0.36; ^1H NMR (400 MHz, CDCl_3) δ 6.76 (1H, s), 6.39 (1H, s), 4.39 (1H, bs), 4.03 (2H, t, $J = 4.4$ Hz), 3.78 (3H, s), 3.69 (3H, s), 3.62 (1H, m), 3.53 (1H, m), 2.54 (2H, t, $J = 4.8$ Hz), 2.15 (3H, m), 1.65-1.87 (4H, m); ^{13}C NMR (100 MHz, CDCl_3) δ 172.5, 170.7, 150.3, 140.5, 140.1, 135.0, 112.3, 110.5, 101.2, 66.5, 59.9, 56.3, 52.4, 50.6, 29.4, 27.5, 23.9, 23.4. m/z (+ESI) calc. for $\text{C}_{18}\text{H}_{26}\text{N}_2\text{O}_6$ (M) $^+$ 366.4 found 367.2 ([M] $^+$).

(S)-Methyl 4-(5-(allyloxycarbonylamino)-4-(2-(hydroxymethyl)pyrrolidine-1-carbonyl)-2-

methoxyphenoxy)butanoate (6). A solution was prepared by dissolving **5** (3.3 g, 9 mmol, 1.0 equiv.) in dry DCM (40 mL). Dry pyridine (1.7 mL, 21.1 mmol, 2.3 equiv.) and a solution of allyl chloroformate (0.91 mL, 8.5 mmol, 0.95 equiv.) in anhydrous DCM (30 mL) were sequentially added to this solution, which was kept at -10°C under N_2 atmosphere. The reaction mixture was left under a magnetic stirrer at room temperature for 2 h, until TLC showed the completion of the reaction. At that point, the reaction mixture was extracted with a saturated CuSO_4 solution (70 mL), saturated aqueous NaHCO_3 (100 mL) and brine (100 mL). The organic phase was dried over MgSO_4 and concentrated under reduced pressure using a rotary evaporator.

The crude of the reaction was subsequently purified by column chromatography (mobile phase: EtOAc, 100%) affording pure **6** (3.6 g, 88%) as a pale yellow solid (m. p. 49 °C)

R_f value (DCM:Acetone 60:40): 0.51; ^1H NMR (400 MHz, CDCl_3) δ 8.72 (1H, bs), 7.77 (1H, s), 6.82 (1H, s), 5.95 (1H, m), 5.35 (1H, dd, $J = 17.2, 1.2$ Hz), 5.23 (1H, dd, $J = 10.0, 0.8$ Hz), 4.63 (2H, dd, $J = 5.6, 1.2$ Hz), 4.40 (1H, bs), 4.11 (2H, t, $J = 4.4$ Hz), 3.82 (3H, s), 3.61 (3H, s), 3.59 (1H, m), 3.50 (1H, m), 2.54 (2H, t, $J = 4.8$ Hz), 2.17 (3H, m), 1.72-1.92 (4H, m); ^{13}C NMR (100 MHz, CDCl_3) δ 173.4, 170.9, 153.6, 150.5, 144.0, 132.3, 131.9, 118.2, 115.7, 111.6, 105.6, 67.7, 66.6, 65.7, 61.6, 60.4, 56.6, 51.7, 30.7, 28.3, 25.1, 24.3. m/z (+ESI) calc. for $\text{C}_{22}\text{H}_{30}\text{N}_2\text{O}_8$ (M) $^+$ 450.4 found 451.2 ($[\text{M}+\text{H}]^+$).

Allyl 11-hydroxy-7-methoxy-8-(4-methoxy-4-oxobutoxy)-5-oxo-2,3,11,11a-hexahydro-1H-pyrrolo[2,1-c][1,4]benzodiazepine-10(5H)-carboxylate (7). BAIB (3.7 g, 11.6 mmol, 1.2 equiv.) and TEMPO (152.0 mg, 1.0 mmol, 0.1 equiv.) were sequentially added to a solution of **6** (4.41 g, 9.7 mmol, 1.0 equiv.) in DCM (200 mL). The reaction was left under a magnetic stirrer for 6 h until TLC showed the completion of the reaction. At that point, the reaction mixture was sequentially washed with saturated sodium metabisulphite (100 mL), saturated aqueous NaHCO_3 (2×100 mL) and brine (100 mL). The organic phase was dried over MgSO_4 and concentrated under reduced pressure using a rotary evaporator. The crude of the reaction was purified by column chromatography (mobile phase: EtOAc/hexane, 50/50, v/v) affording pure **7** (3.3 g, 75%) as a yellow solid (m.p. 74 °C).

R_f value (DCM:Acetone 60:40): 0.51; ^1H NMR (400 MHz, CDCl_3) δ 7.22 (1H, s), 6.69 (1H, s), 5.80 (1H, m), 5.62 (1H, d, $J = 4.0$ Hz), 5.07 (2H, d, $J = 12.0$ Hz), 4.61 (1H, dd, $J = 13.2, 5.6$ Hz), 4.41 (1H, bs), 4.21 (2H, d, $J = 12.0$ Hz), 3.89 (3H, s), 3.67 (3H, s), 3.49 (1H, t, $J = 8.0$ Hz), 3.43

(1H, m), 2.475 (2H, t, $J = 7.2$ Hz), 2.12 (4H, m), 1.95 (2H, m); ^{13}C NMR (100 MHz, CDCl_3) δ 173.4, 167.0, 155.9, 149.9, 148.7, 131.8, 128.3, 126.0, 117.9, 114.2, 110.8, 85.9, 67.9, 66.7, 60.3, 60.1, 56.1, 51.6, 46.3, 30.3, 28.7, 24.2, 23.0, 20.9. m/z (+ESI) calc. for $\text{C}_{22}\text{H}_{28}\text{N}_2\text{O}_8$ (M) $^+$ 448.4 found 449.2 ([M] $^+$ H).

Allyl 7-methoxy-8-(4-methoxy-4-oxobutoxy)-5-oxo-11-(tetrahydro-2H-pyran-2-yloxy)-2,3,11,11a-hexahydro-1H-pyrrolo[2,1-c][1,4]benzodiazepine-10(5H)-carboxylate (8). DHP (6.3 mL, 75.0 mmol, 10.0 equiv.) was added to a solution of **7** (3.3 g, 7.5 mmol, 1.0 equiv.) in the presence of a catalytic amount of PTSA (33.0 mg, 0.2 mmol, 0.03 equiv.) in EtOAc (50 mL). The reaction mixture was left under a magnetic stirrer for 2 h until TLC showed the completion of the reaction. At that point the reaction mixture was extracted with saturated aqueous NaHCO_3 (2 \times 50 mL) and brine (50 mL). The organic phase was dried over MgSO_4 , and evaporated using a rotary evaporator under reduced pressure. The crude of the reaction was purified by column chromatography (mobile phase: DCM/acetone, 90/10, v/v) affording pure **8** (3.6 g, 85%) as a yellow solid (m. p. 53 $^\circ\text{C}$).

R_f value (DCM:Acetone 60:40): 0.67; ^1H NMR (400 MHz, CDCl_3) δ 7.19 (1 H, s), 6.88 (1 H, s), 6.60 (1 H, s), 5.68-5.90 (4 H, m), 5.00-5.20 (8 H, m), 4.30-4.70 (4 H, m), 4.05-4.15 (6 H, m), 3.80-3.92 (8 H, m), 3.62-3.73 (8 H, m), 3.40- 3.55 (8 H, m), 2.50-2.64 (4 H, m), 2.90-2.10 (8H, m), 1.65-1.84 (6 H, m), 1.42-1.62 (15 H, m); ^{13}C NMR (100 MHz, CDCl_3) δ 173.4, 167.4, 149.1, 132.0, 114.9, 100.0, 98.4, 96.1, 94.6, 91.7, 88.6, 68.0, 67.7, 66.5, 63.6, 62.9, 60.1, 56.1, 51.6, 51.2, 46.3, 30.9, 30.2, 29.0, 25.4, 24.2, 20.0. m/z (+ESI) calc. for $\text{C}_{27}\text{H}_{36}\text{N}_2\text{O}_9$ (M) $^+$ 532.5 found 533.2 ([M] $^+$ H).

4-(10-(Allyloxycarbonyl)-7-methoxy-5-oxo-11-(tetrahydro-2H-pyran-2-yloxy)-**2,3,5,10,11,11a-hexahydro-1H- pyrrolo[2,1-c][1,4]benzodiazepine-8-yloxy)butanoic acid (9).**

An excess of NaOH 1 M aqueous solution was added to a solution of **8** (3.8 g, 7.1 mmol, 1.0 equiv.) in MeOH (60 mL). The reaction mixture was left under a magnetic stirrer overnight until TLC showed the completion of the reaction. MeOH was evaporated under reduced pressure using a rotary evaporator and H₂O (30 mL) was added to the residue. Citric acid 1 M aqueous solution was added until acidic pH was reached. The aqueous layer was then extracted with EtOAc (2×50 mL). The combined organic layers were dried over MgSO₄ and concentrated under reduced pressure using a rotary evaporator, giving pure PBD protected acid core **9** (3.2 g, 87%) as a light yellow solid (m. p. 72 °C).

R_f value (DCM:Acetone 60:40): 0.27; ¹H NMR (400 MHz, CDCl₃) δ 7.20 (2 H, s), 6.89 (1 H, s), 6.58 (1 H, s), 5.87 (2 H, d, *J* = 9.2 Hz), 5.72 (2 H, d, *J* = 9.2 Hz), 4.95-5.18 (5 H, m), 4.30-4.60 (5 H, m), 4.00-4.15 (7 H, m), 3.82-3.91 (7 H, m), 3.42-3.69 (9 H, m), 2.49-2.60 (4 H, m), 1.90-2.20 (12 H, m), 1.67-1.81 (4 H, m), 1.40-1.60 (8 H, m); ¹³C NMR (100 MHz, CDCl₃) δ 177.6, 167.6, 149.8, 132.1, 131.9, 126.7, 117.3, 114.9, 110.8, 100.7, 96.0, 91.7, 88.5, 67.9, 66.6, 63.6, 60.1, 56.1, 46.5, 31.1, 30.3, 28.8, 25.2, 24.1, 23.2, 20.0. *m/z* (+ESI) calc. for C₂₆H₃₄N₂O₉ (M)⁺ 518.5 found 519.2 ([M]+H)⁺.

4-(Benzyloxy)-3-methoxybenzaldehyde (10). Benzylbromide (12.9 mL, 108.4 mmol, 1.1 equiv.) and potassium carbonate (6.8 g, 49.3 mmol, 0.5 equiv.) were added to a solution of vanillin (15.0 g, 98.6 mmol, 1.0 equiv.) in acetone (225 mL). The suspension was stirred under reflux overnight until TLC showed the completion of the reaction. At that point H₂O (5000 mL) was added to the reaction, causing the formation of a precipitate that was filtered and recrystallized from EtOH at 0 °C giving pure **10** (14.9 g, 62%) as a pale yellow solid (m. p. 61 °C).

R_f value (100% DCM): 0.71; ¹H NMR (400 MHz, CDCl₃) δ 9.83 (1H, s), 7.29-7.46 (7H, m), 6.98 (1H, d, *J* = 8.06 Hz), 5.25 (2H, s), 3.94 (3H, s); ¹³C NMR (100 MHz, CDCl₃) δ 191.0, 153.6, 150.1, 136.0, 130.3, 128.7, 128.2, 127.2, 126.6, 112.3, 109.3, 70.9, 56.1. m/z (+ESI) calc. For C₁₅H₁₄O₃ (M)⁺ 242.3 found 242.9 ([M]+H)⁺.

4-(Benzyloxy)-5-methoxy-2-nitrobenzaldehyde (11). A solution of **10** (14.8 g, 61.1 mmol, 1.0 equiv.) in trifluoroacetic acid (18 mL) was added dropwise to a solution of KNO₃ (7.7 g, 76.4 mmol, 1.25 equiv.) in trifluoroacetic acid (18 mL) kept at 0°C under magnetic stirrer. After 40 min, the reaction went to completion by TLC and LCMS. The reaction mixture was evaporated under reduced pressure using a rotary evaporator. The residue was dissolved in EtOAc (500 mL), and the organic phase was washed with brine (3×500 mL). The organic phases were dried over MgSO₄ and concentrated by rotary evaporator giving pure **11** (14.5 g, 98%) as a bright yellow solid (m. p. 114 °C).

R_f value (100% DCM): 0.73; ¹H NMR (400 MHz, CDCl₃) δ 10.42 (1H, s), 7.66 (1H, s), 7.34-7.46 (6H, m), 5.26 (2H, s), 4.0 (3H, s); ¹³C NMR (100 MHz, CDCl₃) δ 187.8, 153.7, 151.4,

134.85, 129.0, 128.9, 128.7, 127.6, 125.7, 110.0, 108.9, 71.6, 56.73. m/z (+ESI) calc. For $C_{15}H_{13}NO_5$ (M)⁺ 287.3 found 285.9 ([M]-H)⁻.

4-Hydroxy-5-methoxy-2-nitrobenzaldehyde (12). A solution of **11** (14.4g, 50.1 mmol, 1 equiv.) in acetic acid (120 mL) was heated up to 85°C, and a hydrobromic acid solution 48% (40 mL) was added. The mixture was kept under a magnetic stirrer for 1 h. The solid product obtained was filtered and recrystallized from hot EtOH. The solid obtained was dried in a vacuum oven giving pure **12** (6.1 g 62%) as a yellow solid (m. p. 212 °C).

R_f value (100% DCM): 0.51; ¹H NMR (400 MHz, DMSO-*d*) δ 11.12 (1H, br. s), 10.16 (1H, s), 7.50 (1H, s), 7.35 (1H, s), 3.94 (3H, s); ¹³C NMR (100 MHz, DMSO-*d*) δ 188.3, 151.8, 151.0, 143.7, 123.4, 111.0, 110.6, 56.31. m/z (+ESI) calc. $C_8H_7NO_5$ (M)⁺ 197.2 found 198.0 ([M]+H)⁺.

tert-Butyl (3-(4-formyl-2-methoxy-5-nitrophenoxy)propyl)carbamate (13). *tert*-Butyl (3-bromopropyl)carbamate (7.1 g, 29.6 mmol, 1.05 equiv.) and potassium carbonate (5.8 g, 42.3 mmol, 1.5 equiv.) were added to a solution of **12** (5.6 g, 28.2 mmol, 1.0 equiv.) in DMF (22 mL). The suspension was stirred at 50 °C for 24 h, until TLC showed the completion of the reaction. At that point, H₂O (500 mL) was added to the reaction, and the product was extracted in EtOAc. The organic solvent was then evaporated using the rotary evaporator, and the compound was purified by flash column chromatography (mobile phase hexane/EtOAc, 80:20, v/v) to give pure **13** (9.3 g, 93%) as a brown oil.

R_f value (100% DCM): 0.68; ¹H NMR (400 MHz, CDCl₃) δ 10.44 (1H, s), 7.59 (1H, s), 7.41 (1H, s), 4.23 (2H, t, *J* = 5.92), 4.01 (3H, s), 3.34-3.43 (2H, m), 2.05-2.13 (2H, m), 1.45 (9H, s); ¹³C NMR (100 MHz, CDCl₃) δ 188.5, 155.6, 152.6, 151.2, 143.5, 124.6, 110.0, 108.1, 77.6, 67.3,

56.4, 35.7, 28.8, 28.1; m/z (+ESI) calc. $C_{16}H_{22}N_2O_7$ (M)⁺ 354.4 found 255.0 ($[M]+H-Boc$)⁺, 377.0 ($[M]+Na$)⁺.

4-(3-((*tert*-Butoxycarbonyl)amino)propoxy)-5-methoxy-2-nitrobenzoic acid (14). Compound **13** (9.2 g, 25.9 mmol, 1.0 equiv.) was dissolved in acetone (500 mL). A hot solution of 10% potassium permanganate (250 mL) was added to the solution of **13** in a flask fitted with a condenser. The reaction mixture was left under reflux until the reaction went to completion (according to TLC). At that point, the reaction mixture was cooled down to room temperature. The brown residue formed was filtered through a celite path and washed with 600 mL hot H₂O. A solution of sodium bisulphite 16% (400 mL) was added to the filtrate, and the pH of the solution was adjusted to 3.5 using concentrated citric acid. The product was then extracted in EtOAc. The organic solvent was removed using the rotary evaporator, giving **14** (8.1 g, 83%) as a yellow solid (m. p. 107 °C).

R_f value (EtOAc:MeOH 50:50): 0.57; ¹H NMR (400 MHz, CDCl₃) δ 7.29 (1H, s), 7.08 (1H, br.s.), 4.10 (2H, t, J = 5.29 Hz), 3.89 (3H, s), 3.31-3.38 (2H, m), 2.02 (2H, quin, J = 5.79 Hz), 1.44 (9H, s); ¹³C NMR (100 MHz, CDCl₃) δ 191.1, 156.2, 152.7, 149.0, 128.7, 127.2, 110.8, 107.6, 79.3, 68.3, 56.5, 38.4, 28.5, 28.4. m/z (+ESI) calc. $C_{16}H_{22}N_2O_8$ (M)⁺ 370.4 found 271.0 ($[M]+H-Boc$)⁺, 393.1 ($[M]+Na$)⁺.

***tert*-Butyl (S)-(3-(4-(2-(hydroxymethyl)pyrrolidine-carbonyl)-2-methoxy-5-nitrophenoxy)propyl)carbamate (15).** A solution was prepared by dissolving **14** (8.0 g, 21.6 mmol, 1.1 equiv.), HBTU (18.6 g, 49.0 mmol, 2.5 equiv.) and DIPEA (10.2 mL, 58.8 mmol, 3 equiv.) in DMF (250 mL). The solution was left under a magnetic stirrer for 20 min. Then (S)-(+)-2-pyrrolidinemethanol (1.93 mL, 19.6 mmol, 1.0 equiv.) was added to the mixture which was kept under magnetic stirring at 50 °C for 15 h until TLC showed the completion of the reaction. At that point water was added to the reaction mixture, and the product was extracted in EtOAc. The organic phase was then, washed with brine and a saturated NaHCO₃ solution. The organic solution was concentrated using a rotary evaporator, and the product was purified by flash column chromatography (mobile phase: from 100% EtOAc to EtOAc/MeOH, 98:2, v/v) to afford pure **15** (3.2 g, 35%) as brown solid (m. p. 68°C).

*R*_f value (EtOAc:MeOH 90:10): 0.42; ¹H NMR (400 MHz, CDCl₃) δ 7.67 (1H, s), 6.79 (1H, s), 4.16 (2H, t, *J* = 5.92 Hz), 3.97 (3H, s), 3.85-3.91 (1H, m), 3.75-3.82 (1H, m), 3.33-3.40 (2H, m), 3.15 (2H, t, *J* = 6.55), 2.12-2.21 (2H, m), 2.03-2.09 (2H, m), 1.68-1.93 (4H, m), 1.44 (9H, s); ¹³C NMR (100 MHz, CDCl₃) δ 200.7, 156.0, 154.7, 153.2, 148.3, 127.9, 109.0, 108.0, 79.2, 68.4, 61.6, 56.7, 49.5, 38.5, 29.1, 28.5, 24.4. *m/z* (+ESI) calc. C₂₁H₃₁N₃O₈ (M)⁺ 453.5 found 454.1 ([M]+H)⁺.

***tert*-Butyl (S)-(3-(5-amino-4-(2-(hydroxymethyl)pyrrolidine-1-carbonyl)-2-methoxyphenoxy)propyl)carbamate (16).** A catalytic amount of Pd/C (10% w/w) was added to a solution of **15** (3.2 g, 7.1 mmol, 1.0 equiv.) in EtOH (30 mL). The reaction mixture was hydrogenated in a Parr hydrogenator at 40 psi overnight until TLC showed the completion of the

reaction. At that point, the reaction was filtered under vacuum through a path of celite. The resulting solution was evaporated using rotary evaporator giving pure **16** (2.9 g, 96%) as a yellow solid (m. p. 73 °C).

R_f value (EtOAc:MeOH 90:10): 0.65; ^1H NMR (400 MHz, CDCl_3) δ 6.72 (1H, s), 6.23 (1H, s), 4.04 (2H, t, $J = 5.79$ Hz), 3.79 (3H, s), 3.57-3.71 (2H, m), 3.51 (2H, td, $J = 10.13$, 6.42 Hz), 3.30-3.39 (2H, m), 2.10-2.20 (1H, m), 2.00 (2H, quin, $J = 5.85$ Hz), 1.58-1.93 (4H, m), 1.45 (9H, s); ^{13}C NMR (100 MHz, $(\text{CD}_3)_2\text{SO}$) δ 170.3, 168.5, 155.6, 150.1, 140.0, 112.9, 101.6, 101.2, 77.5, 65.8, 61.4, 61.4, 58.5, 56.4, 37.2, 29.1, 28.2, 27.1, 20.7. m/z (+ESI) calc. $\text{C}_{21}\text{H}_{33}\text{N}_3\text{O}_6$ (M) $^+$ 423.5 found 424.1 ($[\text{M}]+\text{H}$).

***tert*-Butyl (S)-(3-(5-(((allyloxy)carbonyl)amino)-4-(2-(hydroxymethyl)pyrrolidine-1-carbonyl)-2-methoxyphenoxy)propyl)carbamate (17).** A solution was prepared by dissolving **16** (2.8 g, 6.6 mmol, 1.0 equiv.) in dry DCM (82 mL). Dry pyridine (1.42 mL) and a solution of allyl chloroformate (0.67 mL, 6.3 mmol, 0.95 equiv.) in anhydrous DCM (57.38 mL) were sequentially added to this solution, which was kept at -10 °C under an N_2 atmosphere. The reaction mixture was left under a magnetic stirrer at room temperature for 2 h, until TLC showed the completion of the reaction. At that point, the reaction mixture was extracted with a saturated CuSO_4 solution (100 mL), saturated aqueous NaHCO_3 (200 mL) and brine (200 mL). The organic phase was dried over MgSO_4 and concentrated under reduced pressure using a rotary evaporator. Pure **17** (3.1 g, 94%) was obtained as a brown solid (m. p. 47 °C).

R_f value (EtOAc:MeOH 90:10): 0.54; ^1H NMR (400 MHz, CDCl_3) δ 7.73 (1H, dr.s.), 6.80 (1H, s), 5.87-6.01 (1H, m), 5.34 (1H, dd, $J = 17.37, 1.51$ Hz), 5.23 (1H, dd, $J = 10.32, 1.26$ Hz), 4.62

(2H, dq, $J = 5.70, 1.46$ Hz), 4.13 (2H, t, $J = 5.67$ Hz), 3.83 (3H, s), 3.39-3.75 (4H, m), 3.34 (2H, q, $J = 5.71$), 2.10-2.20 (1H, m), 2.01 (2H, quin, $J = 5.85$ Hz), 1.86-1.91 (2H, m), 1.60-1.79 (2H, m), 1.44 (9H, s); ^{13}C NMR (100 MHz, CDCl_3) δ 170.9, 156.1, 153.7, 150.3, 144.0, 132.5, 131.8, 118.2, 110.9, 105.4, 78.9, 68.0, 66.5, 65.8, 61.1, 56.3, 51.6, 38.8, 29.1, 28.5, 28.3, 25.15. m/z (+ESI) calc. $\text{C}_{25}\text{H}_{37}\text{N}_3\text{O}_8$ (M) $^+$ 507.6 found 508.2 ([M]+H) $^+$.

Allyl-8(3-((*tert*-butoycarbonyl)amino)propoxy)-11-hydroxy-7-methoxy-5-oxo-2,3,11,11a-tetrahydro-1*H*-benzo[e]pyrrolo[1,2- α][1,4]diazepine-10-(5*H*)carboxylate (18). BAIB (2.4 g, 7.4 mmol, 1.2 equiv.) and TEMPO (0.1 g, 0.6 mmol, 0.1 equiv.) were sequentially added to a solution of **17** (3.14 g, 6.2 mmol, 1 equiv.) in DCM (160 mL). The reaction was stirred for 6 h until TLC showed the completion of the reaction. At that point, the reaction mixture was sequentially washed with saturated sodium metabisulphite (100 mL), saturated aqueous NaHCO_3 (2 \times 100 mL) and brine (100 mL). The organic phase was dried over MgSO_4 and concentrated under reduced pressure using a rotary evaporator. The crude of the reaction was purified by column chromatography (mobile phase: EtOAc/DCM, 50/50, v/v) affording pure **18** (3 g, 96%) as an ochre solid (m. p. 75 $^\circ\text{C}$).

R_f value (EtOAc:MeOH 90:10): 0.48; ^1H NMR (400 MHz, CDCl_3) δ 7.22 (1H, s), 6.65 (1H, s), 5.69-5.84 (1H, m), 5.57-5.65 (1H, m), 5.46 (1H, br.s.), 4.64 (1H, dd, $J = 13.35, 5.04$ Hz), 4.42 (1H, dd, 13.35, 4.28 Hz), 4.01-4.07 (2H, m), 3.90 (3H, s), 3.64-3.71 (1H, m), 3.41-3.57 (2H, m), 3.32 (2H, d, $J = 5.29$ Hz), 2.06-2.13 (2H, m), 1.87-2.02 (5H, m), 1.43 (9H, s); ^{13}C NMR (100 MHz, CDCl_3) δ 166.9, 156.1, 155.9, 149.8, 148.6, 131.8, 128.4, 126.1, 118.0, 113.7, 110.5, 86.0, 79.0, 68.2, 66.7, 60.0, 56.0, 53.5, 46.4, 38.8, 29.1, 28.7, 28.5, 23.0. m/z (+ESI) calc. $\text{C}_{25}\text{H}_{35}\text{N}_3\text{O}_8$ (M) $^+$ 505.6 found 506.2 ([M]+H) $^+$.

1
2
3
4
5
6
7
8
9
10
11
12
13
14
15
16
17
18
19
20
21
22
23
24
25
26
27
28
29
30
31
32
33
34
35
36
37
38
39
40
41
42
43
44
45
46
47
48
49
50
51
52
53
54
55
56
57
58
59
60

General procedure adopted for amide coupling reactions of the biaryl moieties (19-24).

DMAP (3 equiv.) and EDCI (2 equiv.) were added to a solution of carboxylic acid in DMF (6 mL). The mixture was kept under N₂ atmosphere and magnetic stirring for 30 min. Subsequently, the amino compound (1.5 equiv.) was added to the solution, which was left under a magnetic stirrer at room temperature overnight. An aqueous solution of citric acid at pH = 2.5 (40 mL) was added to the mixture, and the product was extracted with EtOAc. The organic phase was washed with brine and concentrated using a rotary evaporator. The crude product was purified by flash column chromatography (mobile phase: from DCM 100%, to DCM/acetone, 70/30, v/v).

***tert*-Butyl (5-(benzofuran-5-ylcarbamoyl)-1methyl-1*H*-pyrrol-3-yl)carbamate (19).**

330.0 mg, (67%) as pale brown solid (m.p. 176 °C).

*R*_f value (DCM:Acetone 80:20): 0.71; ¹H NMR (400 MHz, CDCl₃) δ 7.89 (1H, d, *J* = 1.51 Hz), 7.81 (1H, br.s.), 7.58 (1H, d, *J* = 2.27 Hz), 7.39 (1H, d, *J* = 8.56 Hz), 7.24 (1H, d, *J* = 8.5 6Hz), 6.83 (1H, s), 6.68 (1H, dd, *J* = 2.14, 0.88 Hz), 6.63 (1H, s), 6.47 (1H, s), 3.85 (3H, s), 1.49 (9H, s); ¹³C NMR (100 MHz, CDCl₃) δ 160.0, 153.6, 151.8, 145.8, 133.0, 127.8, 123.5, 121.8, 118.7, 117.9, 113.2, 111.4, 106.8, 103.9, 80.3, 36.7, 28.4. *m/z* (+ESI) calc. for C₁₉H₂₁N₃O₄ (M)⁺ 355.4 found 355.8 ([M]+H)⁺.

***N*-(benzofuran-5-yl)-4-cyano-1-methyl-1*H*-pyrrole-2-carboxamide (20).** 429.0 mg, (79%) as yellow solid (m.p. 172 °C).

*R*_f value (DCM:Acetone 80:20): 0.69; ¹H NMR (400 MHz, CDCl₃) δ 7.92 (1H, d, *J* = 2.27 Hz), 7.80 (1H, s), 7.64 (1H, d, *J* = 2.01 Hz), 7.48 (1H, d, *J* = 8.81), 7.31 (1H, dd, *J* = 8.69, 2.14 Hz), 7.24 (1H, d, *J* = 1.76 Hz), 6.99 (1H, d, *J* = 1.51 Hz), 6.76 (1H, dd, *J* = 2.27, 1.01 Hz), 4.01 (3H,

s); ^{13}C NMR (100 MHz, CDCl_3) δ 158.6, 152.2, 146.1, 133.6, 132.3, 128.0, 127.5, 118.0, 115.6, 114.7, 113.5, 111.7, 106.8, 92.1, 37.7. m/z (+ESI) calc. for $\text{C}_{15}\text{H}_{11}\text{N}_3\text{O}_2$ (M) $^-$ 265.3 found 263.9 ($[\text{M}]-\text{H}$) $^-$.

Methyl 4-(benzofuran-5-carboxamido)-1-methyl-1*H*-pyrrole-2-carboxylate (21). 144.0 mg, (20%) as dark yellow solid (m.p. 163 °C).

R_f value (DCM:Acetone 80:20): 0.63; ^1H NMR (400 MHz, CDCl_3) δ 8.12 (1H, d, J = 1.51 Hz), 7.89 (1H, s), 7.79 (1H, dd, J = 8.69, 1.64 Hz), 7.70 (1H, d, J = 2.27 Hz), 7.55 (2H, dd, J = 4.91, 3.15 Hz), 6.83 (1H, d, J = 2.27 Hz), 6.80 (1H, d, J = 1.76 Hz), 3.91 (3H, s), 3.81 (3H, s); ^{13}C NMR (100 MHz, CDCl_3) δ 165.0, 161.5, 156.6, 146.4, 129.5, 127.7, 123.4, 121.9, 121.4, 120.7, 119.8, 111.6, 108.2, 107.0, 51.2, 36.9. m/z (+ESI) calc. for $\text{C}_{16}\text{H}_{14}\text{N}_2\text{O}_4$ (M) $^+$ 298.3 found 299.1 ($[\text{M}]+\text{H}$) $^+$.

***tert*-Butyl (5-(benzo[*b*]thiophene-5-ylcarbamoyl)-1-methyl-1*H*-pyrrol-3-yl)carbamate (22).**

435.0 mg, (93%) as brown solid (m. p. 164 °C).

R_f value (DCM:Acetone 80:20): 0.7; ^1H NMR (400 MHz, CDCl_3) δ 8.21 (1H, d, J = 2.01 Hz), 7.80 (1H, d, J = 8.81), 7.70 (1H, s), 7.45 (1H, d, J = 5.29 Hz), 7.35 (1H, dd, J = 8.81, 2.01 Hz), 7.29 (1H, d, J = 5.54 Hz), 6.86 (1H, s), 6.67 (1H, s), 6.29 (1H, br.s.), 3.92 (3H, s), 1.51 (9H, s); ^{13}C NMR (100 MHz, CDCl_3) δ 159.7, 153.5, 140.3, 135.3, 134.7, 127.5, 124.0, 123.5, 122.7, 121.8, 118.7, 117.7, 114.6, 103.8, 80.4, 36.8, 28.4. m/z (+ESI) calc. for $\text{C}_{19}\text{H}_{21}\text{N}_3\text{O}_3\text{S}$ (M) $^+$ 371.5 found 372.0 ($[\text{M}]+\text{H}$) $^+$.

***N*-(benzo[*b*]thiophene-5-yl)-4-cyano-1-methyl-1*H*-pyrrole-2-carboxamide (23).** 970.3 mg, (92%) as brown solid (m.p. 173 °C).

R_f value (DCM:Acetone 80:20): 0.66; ¹H NMR (400 MHz, CDCl₃) δ 8.20 (1H, d, *J* = 2.01 Hz), 7.39 (1H, br.s.), 7.83 (1H, d, *J* = 8.56 Hz), 7.48 (1H, d, *J* = 5.54 Hz), 7.39 (1H, dd, *J* = 8.69, 2.14 Hz), 7.30 (1H, d, *J* = 5.29 Hz), 7.24 (1H, d, *J* = 1.74 Hz), 7.02 (1H, d, *J* = 1.51 Hz), 4.01 (3H, s); ¹³C NMR (100 MHz, CDCl₃) δ 158.6, 140.2, 136.0, 134.1, 133.7, 127.8, 127.4, 123.9, 122.9, 117.9, 115.5, 115.1, 114.8, 92.1, 37.7. *m/z* (+ESI) calc. for C₁₅H₁₁N₃OS (M)⁺ 281.3 found 281.9 ([M]+H)⁺.

Methyl 4-benzo[*b*]thiophene-5-carboxamido)-1-methyl-1*H*-pyrrole-2-carboxylate (24).

390.0 mg, (88%) as white solid (m. p. 214 °C).

R_f value (DCM:Acetone 80:20): 0.65; ^1H NMR (400 MHz, CDCl_3) δ 8.28-8.30 (2H, m), 7.84-7.89 (1H, m), 7.77 (1H, dd, $J = 8.56, 1.76$ Hz), 7.52 (1H, d, $J = 2.01$ Hz), 7.49 (1H, d, $J = 5.54$ Hz), 7.32 (1H, d, $J = 5.29$ Hz), 6.83 (1H, d, $J = 2.01$ Hz), 3.86 (3H, s), 3.78 (3H, s); ^{13}C NMR (100 MHz, CDCl_3) δ 165.0, 161.5, 142.8, 139.5, 130.6, 128.0, 124.2, 122.7, 122.6, 122.34, 121.9, 121.4, 119.9, 108.4, 51.2, 36.9. m/z (+ESI) calc. for $\text{C}_{16}\text{H}_{14}\text{N}_2\text{O}_3\text{S}$ (M) $^+$ 314.4 found 314.9 ([M]+H) $^+$.

General procedure adopted for the nitrile hydrolysis (25, 26). The biaryl compound bearing the nitrile group was solubilized in a mixture of dioxane (4 mL) and water (10 mL), and concentrated H_2SO_4 (2 mL) was added to this mixture. The solution was kept under magnetic stirring at 80°C for 96 h. A saturated solution of NaHCO_3 was slowly added until the mixture reached pH = 8, and then it was washed with EtOAc (250 mL). The concentrated HCl was added to the aqueous phase to reach pH = 2 and the product was extracted with EtOAc (300 mL). The organic phase was concentrated using a rotary evaporator, and the crude product was purified by flash column chromatography (mobile phase: from 100% EtOAc to EtOAc/MeOH, 95/5, v/v).

5-(Benzofuran-5-ylcarbamoyl)-1-methyl-1*H*-pyrrole-3-carboxylic acid (25). 39.0 mg, (9%) as brown solid (186 °C).

R_f value (Acetone:DCM 80:20): 0.37; ^1H NMR (400 MHz, $(\text{CD}_3)_2\text{SO}$) δ 10.03 (1H, s), 8.09 (1H, d, $J = 1.51$ Hz), 7.69 (1H, d, $J = 2.01$ Hz), 7.51-7.56 (3H, m), 7.37 (1H, d, $J = 1.76$ Hz), 6.95 (1H, d, $J = 1.51$ Hz), 3.88 (3H, s); ^{13}C NMR (100 MHz, $\text{CH}_3\text{OD}-d$) δ 162.0, 153.5, 147.3, 134.7, 134.0, 129.1, 128.4, 120.0, 116.0, 115.7, 115.1, 112.0, 107.8. m/z (+ESI) calc. for $\text{C}_{15}\text{H}_{12}\text{N}_2\text{O}_4$ (M^-) 284.3 found 283.0 ($[\text{M}]-\text{H}$) $^-$.

5-(Benzo[*b*]thiophene-5-ylcarbamoyl)-1-methyl-1*H*-pyrrole-3-carboxylic acid (26). 85.0 mg, (7%) as brown solid (181 °C).

R_f value (Acetone:DCM 80:20): 0.39; ^1H NMR (400 MHz, $\text{CD}_3\text{OD}-d$) δ 8.20 (1H, d, $J = 1.76$ Hz), 7.85 (1H, d, $J = 8.81$ Hz), 7.52-7.59 (3H, m), 7.38 (1H, $J = 1.76$ Hz), 7.34 (1H, d, $J = 4.78$ Hz), 3.99 (3H, s); ^{13}C NMR (100 MHz, $\text{CD}_3\text{OD}-d$) δ 141.6, 136.9, 136.5, 134.1, 128.5, 124.9, 123.4, 119.9, 116.6, 116.1, 115.8. m/z (+ESI) calc. for $\text{C}_{15}\text{H}_{12}\text{N}_2\text{O}_3\text{S}$ (M^-) 300.3 found 301.0 ($[\text{M}]+\text{H}$) $^+$.

General procedure adopted for Boc-deprotection (18, 19, 22). The Boc-protected compound was added to a mixture of DCM (2 mL) and TFA (1 mL) and kept under a magnetic stirrer for 30 min. The organic solvent was then evaporated under vacuum.

General procedure for methyl ester hydrolysis (21, 24). The compound bearing the methyl ester was solubilized in a mixture of H₂O (10 mL), and dioxane (2 mL) and an excess of NaOH was added. The solution was kept under magnetic stirring for 5 h until the completion of the reaction. The dioxane was then eliminated under vacuum at the rotary evaporator, and HCl was added to the aqueous solution to reach pH = 2. The product was subsequently extracted with EtOAc (50 mL), and the organic solvent was evaporated using a rotary evaporator.

General procedure adopted for the amide coupling between PBD core and biaryl moiety and for the final deprotection (27-32). The moiety bearing the carboxylic acid was dissolved in DMF (4 mL), and DMAP (3 equiv.) and EDCI (2 equiv.) were added to the solution, which was left under a magnetic stirrer for 30 min. The amino compound was then added to the mixture, which was kept in an N₂ atmosphere and was stirred at room temperature overnight at which point TLC showed the completion of the reaction. Then an aqueous solution of citric acid (100 mL) at pH = 2 was added and the product was extracted with EtOAc (100 mL). The solvent was evaporated under vacuum, and the product was purified by flash column chromatography (mobile phase: from DCM 100% to DCM/acetone, 60:40, v/v). The compound obtained was dissolved in DCM (3 mL), and Pd(PPh₃)₄ (0,05 equiv.), triphenylphosphine (0.25 equiv.) and pyrrolidine (1.2 equiv.) were added. The solution was left under a magnetic stirrer for 30 min, and then the solvent was evaporated using a rotary evaporator. The obtained solid was kept under high vacuum for 15 min, and the product was finally purified through flash column chromatography (mobile phase: from DCM 100% to DCM/acetone, 40:60, v/v).

(S)-N-(Benzofuran-5-yl)-4-(4-((7-methoxy-5-oxo-2,3,5,11a-tetrahydro-1H-benzo[e]pyrrolo[1,2-a][1,4]diazepin-8-yl)oxy)butanamido)-1-methyl-1H-pyrrole-2-carboxamide (27). 38.0 mg, (38%) as white solid (m.p. 144 °C).

R_f value (DCM:Acetone 20:80): 0.25 ; ^1H NMR (400 MHz, CDCl_3) δ 8.19 (1H, s), 8.13 (1H, s), 7.92 (1H, d, $J = 2.01$ Hz), 7.62 (1H, d, $J = 4.28$ Hz), 7.57 (1H, d, $J = 2.27$ Hz), 7.47 (1H, s), 7.31-7.41 (1H, m), 7.30 (1H, m), 7.09 (1H, d, $J = 1.76$ Hz), 6.68 (1H, dd, $J = 2.14, 0.88$ Hz), 6.57 (1H, d, $J = 1.76$ Hz), 4.05 (2H, t, $J = 6.04$ Hz), 3.85 (3H, s), 3.82 (3H, s), 3.72-3.79 (1H, m), 3.64-3.69 (1H, m), 3.50-3.54 (1H, m), 2.44-2.50 (2H, m), 2.16-2.33 (4H, m), 1.95-2.06 (3H, m); ^{13}C NMR (100 MHz, CDCl_3) δ 168.9, 163.6, 161.8, 159.0, 150.7, 149.6, 146.6, 144.7, 139.6, 132.2, 126.73, 122.2, 120.5, 119.3, 118.6, 117.0, 112.2, 110.6, 110.3, 109.7, 105.8, 103.0, 67.0, 55.0, 52.7, 45.7, 35.7, 29.9, 28.2, 23.9, 23.1; IR (FT/IR, ν_{max} / cm^{-1}): 1600, 1468, 1433, 1263, 1200, 1228, 760, 733; HRMS (EI, m/z): calc for $\text{C}_{31}\text{H}_{31}\text{N}_5\text{O}_6$ (M), 570.2347; found, 570.2340.

(S)-N2-(benzofuran-5-yl)-N4-(3-((7-methoxy-5-oxo-2,3,5,11a-tetrahydro-1H-benzo[e]pyrrolo[1,2-a][1,4]diazepin-8-yl)oxy)propyl)-1-methyl-1H-pyrrole-2,4-dicarboxamide (28). 9.0 mg, (14%) as white solid (m.p. 135 °C).

R_f value (EtOAc:Methanol 95:5): 0.23; ^1H NMR (400 MHz, CDCl_3) δ 8.18 (1H, br. s), 7.95 (1H, d, $J = 1.51$ Hz), 7.65 (1H, d, 4.28 Hz), 7.61 (1H, d, $J = 2.27$ Hz), 7.52 (1H, s), 7.45 (1H, d, $J = 8.81$ Hz), 7.34 (1H, dd, $J = 8.31, 1.51$ Hz), 7.29 (1H, s), 7.15 (1H, br.s), 6.83 (1H, s), 6.79 (1H, br. s), 6.75 (1H, d, $J = 2.01$ Hz), 4.21-4.29 (1H, m), 4.11-4.18 (1H, m), 3.98 (3H, s), 3.86 (3H, s), 3.76-3.80 (1H, m), 3.53-3.72 (4H, m), 2.26-2.33 (2H, m), 1.94-2.07 (4H, m); ^{13}C NMR (100 MHz, CDCl_3) δ 163.9, 162.9, 159.7, 152.0, 150.5, 147.5, 145.9, 141.0, 132.9, 129.5, 127.9, 126.7, 120.6, 118.7, 117.9, 113.2, 112.3, 111.6, 111.0, 110.5, 106.9, 68.7, 56.4, 53.8, 53.7, 46.7,

37.3, 29.6, 29.3, 24.2; IR (FT/IR, ν_{\max} / cm^{-1}): 1572, 1263, 1215, 1200, 1084, 1026, 760, 623;
HRMS (EI, m/z): calc for $\text{C}_{31}\text{H}_{31}\text{N}_5\text{O}_6$ (M), 570.2347; found, 570.2344.

(S)-4-(Benzofuran-5-carboxamido)-N-(3-((7-methoxy-5-oxo-2,3,5,11a-tetrahydro-1H-benzo[e]pyrrolo[1,2-a][1,4]diazepin-8-yl)oxy)propyl)-1-methyl-1H-pyrrole-2-carboxamide (29). 20.0 mg, (22%) as white solid (m.p. 139 °C).

R_f value (DCM:Acetone 20:80): 0.26; ^1H NMR (400 MHz, CDCl_3) δ 8.71 (1H, s), 8.19 (1H, d, $J = 1.76$ Hz), 7.87 (1H, dd, $J = 8.81, 1.76$ Hz), 7.66 (1H, d, 2.27 Hz), 7.63 (1H, d, $J = 4.53$ Hz), 7.51 (1H, d, $J = 8.56$ Hz), 7.44 (1H, s), 7.35 (1H, d, $J = 1.76$ Hz), 6.79 (1H, dd, $J = 2.27, 0.76$ Hz), 6.72-6.77 (2H, m), 6.52 (1H, d, $J = 1.76$ Hz), 4.16-4.23 (1H, m), 4.06-4.10 (1H, m), 3.86 (3H, s), 3.74-3.82 (4H, m), 3.60-3.68 (2H, M), 3.49-3.56 (2H, m), 2.24-2.32 (2H, m), 1.99-2.10 (4H, m); ^{13}C NMR (100 MHz, CDCl_3) δ 165.0, 164.6, 162.6, 161.8, 156.5, 150.4, 147.6, 146.3, 140.6, 129.6, 127.6, 123.7, 123.5, 121.7, 120.9, 120.4, 119.3, 111.4, 110.4, 107.1, 103.6, 68.4, 55.9, 53.8, 46.7, 37.4, 36.5, 29.6, 29.3, 24.2; IR (FT/IR, ν_{\max} / cm^{-1}): 1599, 1433, 1410, 1265, 1198, 1142, 812, 731, 623; HRMS (EI, m/z): calc for $\text{C}_{31}\text{H}_{31}\text{N}_5\text{O}_6$ (M), 570.2347; found, 570.2344.

(S)-N-(Benzo[b]thiophen-5-yl)-4-(4-((7-methoxy-5-oxo-2,3,5,11a-tetrahydro-1H-benzo[e]pyrrolo[1,2-a][1,4]diazepin-8-yl)oxy)butanamido)-1-methyl-1H-pyrrole-2-carboxamide (30). 60.0 mg, (57%) as white solid (m.p. 139 °C).

R_f value (DCM:Acetone 20:80): 0.28; ^1H NMR (400 MHz, $(\text{CD}_3)_2\text{SO}$) δ 9.93 (2H, d, $J = 2.27$ Hz), 8.35 (1H, d, $J = 2.01$ Hz), 7.90 (1H, d, $J = 8.81$ Hz), 7.78 (1H, d, $J = 4.28$ Hz), 7.74 (1H, d, $J = 5.54$ Hz), 7.63 (1H, dd, $J = 8.69, 1.89$ Hz), 7.42 (1H, d, $J = 5.29$ Hz), 7.33 (1H,

1
2
3 s), 7.24 (1H, d, $J = 1.76$ Hz), 7.00 (1H, d, $J = 1.76$ Hz), 6.83 (1H, s), 4.09-4.18 (1H, m),
4
5 3.99-4.08 (1H, m), 3.85 (3H, s), 3.83 (3H, s), 3.56-3.42 (1H, m), 2.45 (2H, t, $J = 7.43$ Hz),
6
7 2.14-2.31 (2H, m), 2.00-2.08 (2H, m), 1.87-1.96 (2H, m); ^{13}C NMR (100 MHz, $(\text{CD}_3)_2\text{SO}$) δ
8
9 168.8, 164.2, 163.3, 159.8, 150.1, 146.9, 140.5, 139.7, 136.2, 133.6, 127.9, 124.0, 122.6, 122.3,
10
11 122.0, 119.8, 118.8, 118.2, 114.4, 111.1, 110.0, 104.8, 67.7, 55.5, 53.4, 46.3, 36.2, 31.9, 28.8,
12
13 24.7, 23.6; IR (FT/IR, ν_{max} / cm^{-1}): 1620, 1595, 1261, 1198, 1157, 1020, 874, 768, 692, 581;
14
15 HRMS (EI, m/z): calcd for $\text{C}_{31}\text{H}_{31}\text{N}_5\text{O}_5\text{S}_1$ (M), 586.2119; found, 586.2114.
16
17
18
19
20
21
22
23
24
25
26
27
28
29
30
31
32
33
34
35
36
37
38
39
40
41
42
43
44
45
46
47
48
49
50
51
52
53
54
55
56
57
58
59
60

(S)-N2-(Benzo[b]thiophen-5-yl)-N4-(3-((7-methoxy-5-oxo-2,3,5,11a-tetrahydro-1H-benzo[e]pyrrolo[1,2-a][1,4]diazepin-8-yl)oxy)propyl)-1-methyl-1H-pyrrole-2,4-dicarboxamide (31). 8.5 mg, (14%) as a pale yellow solid (m.p. 142 °C).

R_f value (DCM:Acetone 20:80): 0.26; ^1H NMR (400 MHz, CDCl_3) δ 8.26 (1H, br.s), 8.24 (1H, s), 7.80 (2H, dd, $J = 8.44, 5.41$ Hz), 7.65 (1H, d, $J = 3.53$ Hz), 7.52 (1H, s), 7.40-7.47 (2H, m), 7.35 (1H, d, $J = 8.06$ Hz), 7.29 (1H, s), 7.19 (1H, s), 6.82 (1H, dr.s), 4.21-4.30 (1H, m), 4.08-4.18 (1H, m), 3.98 (3H, s), 3.86 (3H, s), 3.75-3.82 (2H, m), 3.51-3.69 (4H, m), 2.25-2.34 (2H, m), 1.93-2.09 (4H, m); ^{13}C NMR (100 MHz, CDCl_3) δ 163.9, 162.8, 160.7, 159.7, 152.0, 147.5, 140.2, 135.5, 129.9, 129.6, 128.1, 127.6, 126.6, 124.0, 122.8, 117.9, 114.8, 112.4, 111.2, 68.7, 56.4, 53.7, 46.7, 37.4, 31.8, 29.7, 29.3, 24.2, 21.7; IR (FT/IR, ν_{max} / cm^{-1}): 1599, 1572, 1431, 1024, 970, 808, 768, 694, 482; HRMS (EI, m/z): calc for $\text{C}_{31}\text{H}_{31}\text{N}_5\text{O}_5\text{S}_1$ (M), 586.2119; found, 586.2116

(S)-4-(Benzo[b]thiophene-5-carboxamido)-N-(3-((7-methoxy-5-oxo-2,3,5,11a-tetrahydro-1H-benzo[e]pyrrolo[1,2-a][1,4]diazepin-8-yl)oxy)propyl)-1-methyl-1H-pyrrole-2-carboxamide (32). 57.0 mg, (36%) as pale yellow solid (m.p. 169 °C).

R_f value (DCM:Acetone 20:80): 0.28; ^1H NMR (400 MHz, CDCl_3) δ 9.27 (1H, s), 8.40 (1H, s), 7.86-7.91 (1H, m), 7.81-7.85 (1H, m), 7.58 (1H, d, $J = 4.28$ Hz), 7.44 (1H, d, $J = 5.54$ Hz), 7.38 (1H, s), 7.33 (1H, d, $J = 1.76$ Hz), 7.28 (1H, d, $J = 5.54$ Hz), 6.79 (1H, t, $J = 5.54$ Hz), 6.70 (1H, s), 6.56 (1H, d, $J = 1.76$ Hz), 4.05-4.13 (1H, m), 3.94-4.02 (1H, m), 3.78 (3H, s), 3.71 (3H, s), 3.41-3.65 (5H, m), 2.23 (2H, t, $J = 6.29$ Hz), 1.90-2.02 (4H, m); ^{13}C NMR (100 MHz, CDCl_3) δ 165.0, 164.7, 162.5, 161.8, 150.4, 147.5, 142.5, 140.5, 139.4, 130.7, 127.7, 124.3, 123.5, 123.0, 122.9, 122.4, 121.9, 120.2, 119.3, 111.3, 110.2, 103.8, 68.3, 55.9, 53.7, 46.7, 37.3, 36.4, 29.5, 29.3, 24.2; IR (FT/IR, ν_{max} / cm^{-1}): 1600, 1431, 1261, 1200, 1161, 869, 810, 694, 606, 482; HRMS (EI, m/z): calc for $\text{C}_{31}\text{H}_{31}\text{N}_5\text{O}_5\text{S}_1$ (M), 586.2119; found, 586.2113.

FRET based DNA melting assay.

The oligonucleotide sequence used for the FRET-based DNA thermal denaturation assays was purchased from Eurogentec, Southampton, UK. Netropsin hydrochloride was purchased from Sigma-Aldrich UK. The working solution of the oligonucleotide solution (400 nM) was prepared in a FRET buffer (optimized as 50 mM potassium, 50 mM cacodylate, pH 7.4). The oligonucleotides were annealed by heating the samples to 85 °C for 6 mins followed by cooling to 25 °C and storing at this temperature for 5 h. Annealed DNA (25 µL) and sample solution (25 µL) were added to each well of a 96-well plate (MJ Research, Waltham, MA), incubated for 3 h and processed in a DNA Engine Opticon (MJ Research). Fluorescence readings were taken at intervals of 0.5 °C over the range 30-100 °C, with a constant temperature maintained for 30 s prior to each reading. The raw data was imported into the Origin program (Version 7.0, OriginLab Corp.), and the graphs were smoothed using a 10-point running average, and then normalized. The determination of melting temperatures was based on values at the maxima of the first derivative of the smoothed melting curves using a script. The difference between the melting temperature of each sample and that of the blank (ΔT_m) was used for comparative purposes.

Eukaryotic toxicity determination

Cell Culture

The HeLa (human cervical cancer) cell line was obtained from the American Type Culture Collection. The HeLa cell line was maintained in Dulbecco's Modified Eagles Media (DMEM; Invitrogen) supplemented with foetal bovine serum (10% v/v; Invitrogen), L-glutamine (2 mM; Invitrogen), non-essential amino acids (1x; Invitrogen) and Penicillin-Streptomycin (1% v/v, Invitrogen). For WI-38, high glucose DMEM (4.5 g/l; Invitrogen), fetal bovine serum (10%, Biosera UK), non-essential amino acids (1x; Invitrogen) and L-glutamine (2 mM; Invitrogen) were used for sub-culturing. During seeding, cells were counted using a Neubauer haemocytometer (Assistant, Germany) by microscopy (Nikon, USA) on a non-adherent suspension of cells that were washed in PBS, trypsinised, centrifuged at 8 °C at 8000 rpm for 5 min and re-suspended in a fresh medium.

MTT Assay

The cells were grown in normal cell culture conditions at 37 °C in a 5% CO₂ humidified atmosphere using the cell-specific medium listed in the cell culture section above. The cell count was adjusted to 10⁵ cells/mL, and 10,000 cells were added per well. The cells were incubated for 24 h and 1 µl of the appropriate ligand concentrations were added to the wells in triplicate. After 24 h of continuous exposure to each compound, the cell viability was determined using the 3-(4,5-Dimethylthiazol-2-yl)-2,5-diphenyltetrazolium bromide (MTT) (Lancaster Synthesis Ltd, UK) colorimetric assay. Absorbance was quantified by spectrophotometry at $\lambda = 570$ nm (Envision Plate Reader, PerkinElmer, USA). Percentage survival values were calculated by a dose-response analysis using the GraphPad Prism® software.

Microbiological Evaluation

Minimum Inhibitory Concentration (MIC). The MIC is the lowest concentration of an antimicrobial that will inhibit the growth of 99% of a microorganism after overnight incubation. The MIC of the synthesized compounds was determined using the broth microdilution method. Bacteria were grown in Tryptic Soy broth (TSB) (Sigma) or on tryptic soy agar (TSA) plates at 37 °C. A solution of 128 µg/ml of the synthesized molecules in water was prepared from a 2 mg/ml stock solution in DMSO and then sequentially diluted by two-fold in a 96 well plate. 100 µl of bacterially infected media at a concentration of 1×10^6 CFU/ml was inoculated in each well (final bacterial conc. of 5×10^5 CFU/ml). The maximum DMSO content in each well after the addition of the media was $\leq 1\%$. The plate was then incubated statically at 37 °C for 20 h and absorbance at a wavelength of 600 nm (OD_{600}) was measured.

Time-kill Kinetics Assay

The bactericidal or bacteriostatic mode of killing was analyzed using a time-kill assay. Briefly, 10 ml of bacteria at a starting concentration of approximately 10^6 CFU/ml was incubated in a glass conical flask in TSB for 24 h at 37 °C with shaking in the presence of the compound at $4 \times$ MIC. At specified time-points, 100 µl was removed from the culture and diluted in PBS using the method of Miles and Misra.³³ 10 µl spots of the dilutions were plated onto TSA plates and incubated overnight at 37 °C to obtain a cell count.

Gyrase Inhibition Assay

The wild-type gyrase and the gyrase with the S84L mutation were treated with compound **29** and the positive control ciprofloxacin using the cell-free *S. aureus* gyrase supercoiling high throughput plate assay (#SATRG01), obtained from Inspiralis (Norwich, UK).³⁴ This assay is based on the fact that negatively-supercoiled plasmids form intermolecular triplex DNA more readily than relaxed plasmids under the experimental condition. The methods were conducted as per the manufacturer's instructions as described previously.³⁵ Briefly, a relaxed pNO1, a modified form of pBR322 which contains a 'triplex-forming sequence' was used as the substrate. Initially the wells were hydrated using 1× wash buffer (20 mM Tris·HCl (pH 7.6), 137 mM NaCl, 0.005% (w/v) bovine serum albumin (acetylated), 0.05% (v/v) Tween-20). This was followed by immobilisation of 100 µl of 500nM TFO1 oligo in each well by incubating for 5 minutes at room temperature. Excess oligo was carefully washed with assay buffer and ultrapure water. 24 µL of mix buffer was prepared by adding 0.75 µL of pNO1, 6 µL of assay buffer (40 mM HEPES, KOH, 10 mM magnesium acetate, 10 mM DTT, 2 mM ATP, 500 mM potassium glutamate, 0.05 mg/ml albumin, pH 7.6) and 17.25 µL ultrapure water. The mix buffer was added to each well. This was followed by addition of 3 µL inhibitor and 3 µL dilution buffer (50 mM Tris.HCl, 1 mM DTT, 1 mM EDTA, 40 % (w/v) glycerol). The plate was incubated at 37 °C for 30 minutes. This was followed by the addition of 100 µL of TF (triplex forming) assay buffer (10mM sodium acetate pH 4.7, 50mM sodium chloride and 50mM magnesium chloride) and incubating the plate for a further period of 30 minutes to allow triplex formation. The wells were washed with 200 µL TF buffer to remove the unbound plasmid. Finally, PR omega diamond dye (in 10 mM Tris-HCl pH8 1 mM EDTA) was added, and the plates were read by a fluorescent plate reader (ex. 495-15, em. 537-20) after 20 minutes of incubation at room temperature in the dark.

Molecular Modelling

Preparation of DNA & compounds structures: Double Strand (DS) DNA type B (BDNA) was generated by NAB module of AMBER 12.0 package program, using the template of the sequences used in the study (AT-rich 5'-TATATAAGATATATATA-3', mixed 5'-TAGCTAGCTAGCTAGCG-3' and GC-rich 5'-GCGCGCGCGCGGCGCGC-3'). PDB files for the ligands were generated by Chem3DPro 13.0. DNA and compounds' structures were minimized by SYBYL software before covalent molecular docking.

Covalent molecular docking: Covalent docking was performed by forming the covalent bond between the exocyclic amine of guanine and the N10-C11 imine of the PBD using the Autodock SMINA.³⁶ C11-S-stereochemistry was maintained in every case at the binding interface of the PBD. All parameters were kept at their default values.

Molecular Dynamics (MD) simulations. After covalent molecular docking, the best poses of each complex were selected as the starting structures to run MD simulations for 10 ns. The MD simulations were carried out using the AMBER 12.0 package program. The force fields parameters for the compounds were generated using the ANTECHAMBER module of AMBER program. Each system was solvated by using an octahedral box of TIP3P water molecules. Periodic boundary conditions and particle-mesh Ewald (PME) method were employed in all the simulations.³⁷ During each simulation, all bonds in which the hydrogen atom was present were considered fixed, and all other bonds were constrained to their equilibrium values by applying the SHAKE algorithm.³⁸ A cutoff radius of 12Å was used for the systems. Minimization was performed in two phases and each phase was performed in two stages. In the first phase, ions and

all water molecules were minimized for 500 cycles of steepest descent followed by 500 cycles of conjugate gradient minimization. Afterwards, the whole systems were minimized for a total of 1000 cycles without restraint wherein 500 cycles of steepest descent were followed by 500 cycles of conjugate gradient minimization. After minimizations, the systems were heated for 100 ps while the temperature was raised from 0 to 300 K, and then equilibration was performed without a restraint for 100 ps while the temperature was kept at 300 K. Sampling of reasonable configurations was conducted by running a 10 ns simulation with a 2 fs time step at 300 K and 1 atm pressure. A constant temperature was maintained by applying the Langevin algorithm while the pressure was controlled by the isotropic position scaling protocol used in AMBER.³⁹

MM-PBSA/MM_GBSA calculation. 20 snapshots were collected from the last 200 ps of simulations of DNA-compound complexes for post-processing analysis. The ΔG_{PB} term was calculated by solving the finite-difference Poisson-Boltzmann equation using the internal PBSA program.⁴⁰ The SCALE value was set to 2. The Parse radii were employed for all atoms. The solvent probe radius was set at 1.4 Å (with the radii in the prmtop files). MM-PBSA running was performed with the pbsa module (PROC=2). The value of the exterior dielectric constant was set at 80, and the solute dielectric constant was set at 1.⁴¹ The nonpolar contribution was determined on the basis of the solvent accessible surface area (SASA) using the LCPO method⁴² and CAVITY-OFFSET set at 0.00.

Molecular docking of the compounds to wild and mutant gyrase A: AutoDock SMINA was used for molecular docking of ciprofloxacin, as a control, and compound **29** to the minimized crystal structure of Gyrase A from *S. aureus* (PDB ID code 2XCT), for finding the best binding

pocket by exploring all probable binding cavities in the enzyme. All the parameters were kept in their default values. Then, GOLD molecular docking was used for molecular docking of the compounds into the SMINA-located binding site for performing flexible molecular docking and determining more precise and evaluated energies and scores. Based on the fitness function score and ligand binding position, the best-docked pose for each compound was selected. The high fitness function score, generated using the GOLD program, with a low binding energy value, reveals the best-docked pose for each system.

In this study, molecular docking of the compounds to the mutant form of gyraseA was performed as well. After altering Ser84 to Leu with a proper rotamer using PyMOL software, the new structure of gyraseA_S84L was minimized by using Sybyl program. For minimization, the method was set to Powell, initial optimization was set to Simplex, termination was set to Gradient 0.01 kcal/(mol*Å), and the maximum interactions was set to 10000. The minimized structure of the mutant enzyme was used to run the molecular docking by GOLD, as explained above, for the wild type. A genetic algorithm (GA) is used in GOLD ligand docking to thoroughly examine the ligand conformational flexibility along with the partial flexibility of the protein. The maximum number of runs was set to 20 for each compound, and the default parameters were selected (100 population size, 5 for the number of islands, 100,000 number of operations and 2 for the niche size). Default cutoff values of 2.5 Å (dH-X) for hydrogen bonds and 4.0 Å for van-der-Waals distance were employed. When the top solutions attained the RMSD values within 1.5 Å°, the GA docking was terminated.

FIGURES

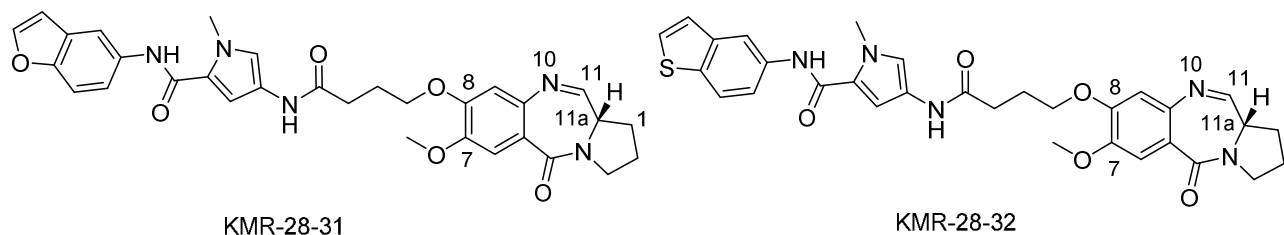


Figure 1. Structure of KMR-28-31 (**27**, PBD-Py-Bzf) and KMR-28-32 (**30**, PBD-Py-Bzt), previously reported C8-benzofused PBDs with antistaphylococcal activity ($\text{MIC} \leq 0.125 \mu\text{g/mL}$).

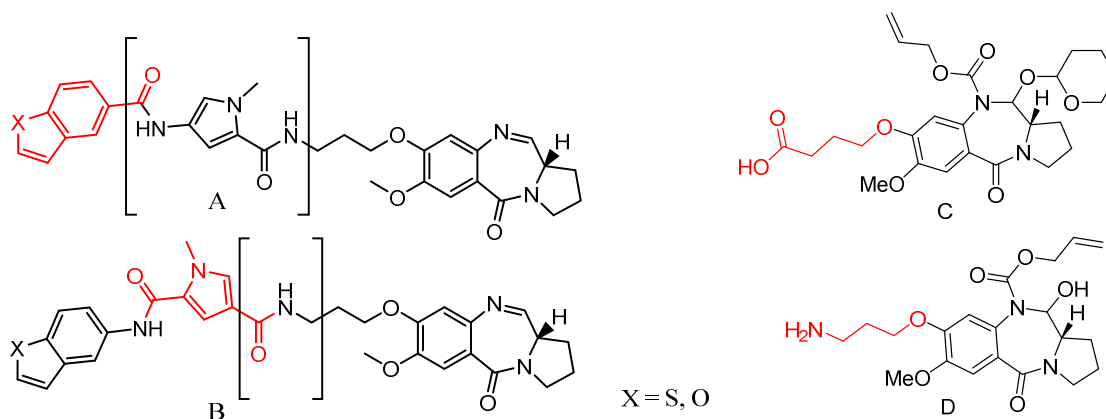


Figure 2. A) & B), Structures showing (in brackets) the reverse moieties and (in red) the different building blocks from the reference compounds; C) Traditional PBD core with 4C-acid linker; D) New PBD core with 4C-amine linker.

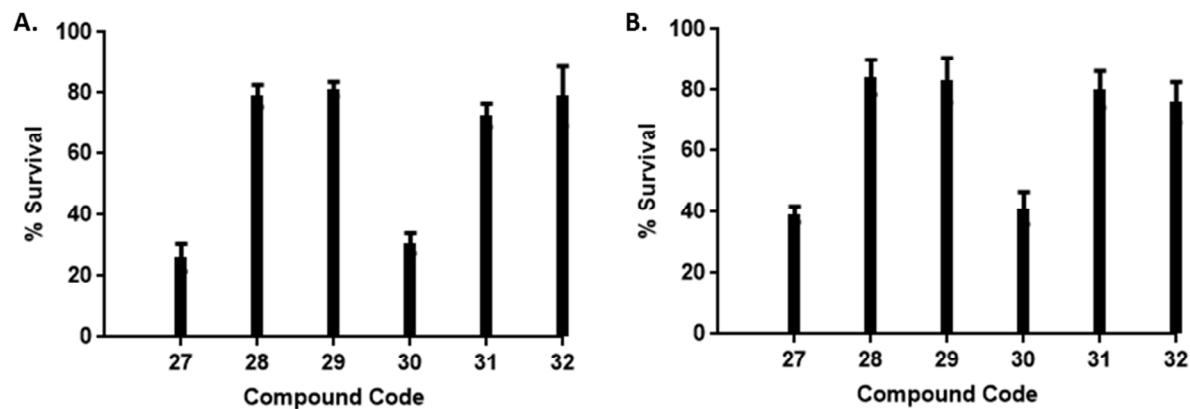


Figure 3. Eukaryotic toxicity of the C8-Benzofused PBDs with natural and inverted building blocks at 25 μ M after 24 h incubation against A) cervical cancer cell line HeLa and B) non-tumour lung fibroblast WI38.

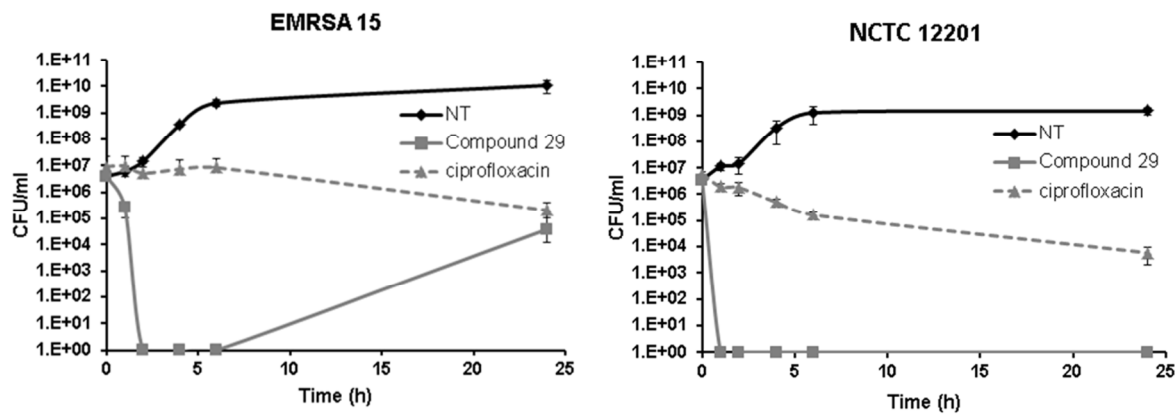


Figure 4. Response of EMRSA-15 and VRE-12201 strains to treatment with suprainhibitory concentrations (4 \times MIC) of compound 29.

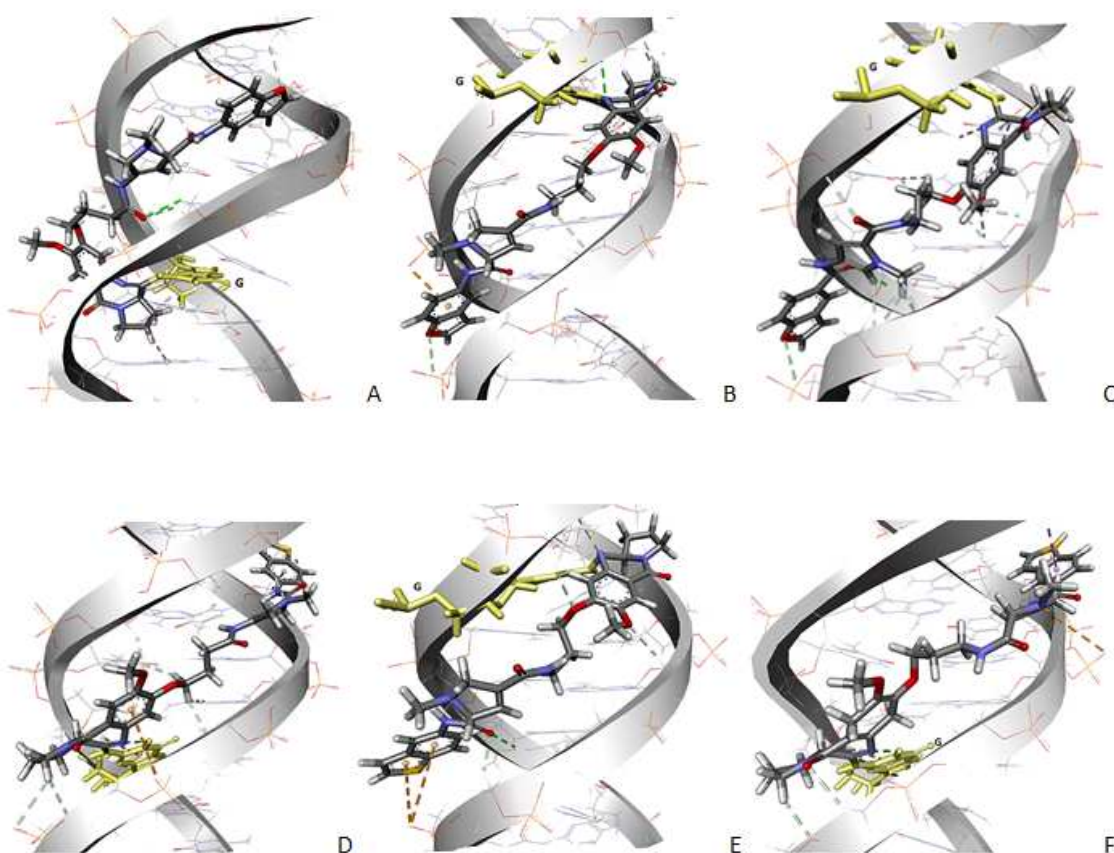


Figure 5. The covalent interactions between a random sequence of DNA and compound **27** (A), **28** (B), **29** (C) in the top panel and with **30** (D), **31** (E) and **32**(F) in the lower panel. All compounds lay along the minor groove of DNA and form covalent interaction to the exocyclic N₂ atom of NH₂ group of a Guanine (in yellow sticks) with their C11 atom present in C=N imine bond.

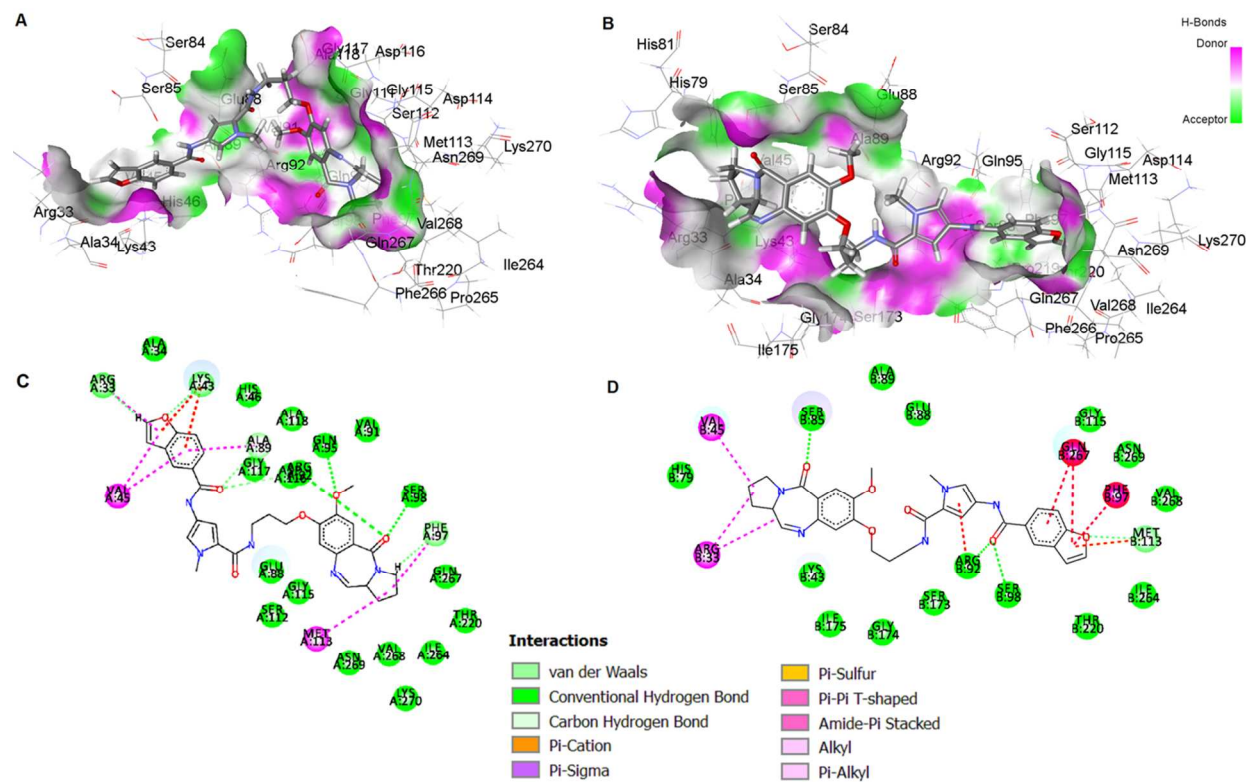


Figure 6. **A)** Molecular model showing the interaction of compound **29** with the subunit-1 of the *S. aureus* gyrase A; **B)** Molecular model showing the interaction of compound **29** with the subunit-2 of the *S. aureus* gyrase A; **C)** 2D model showing the Key interactions between compound **29** with the binding site in the subunit-1 of the *S. aureus* gyrase A; **D)** 2D model showing the key interactions between compound **29** with the binding site in the subunit-2 of the *S. aureus* gyrase A.

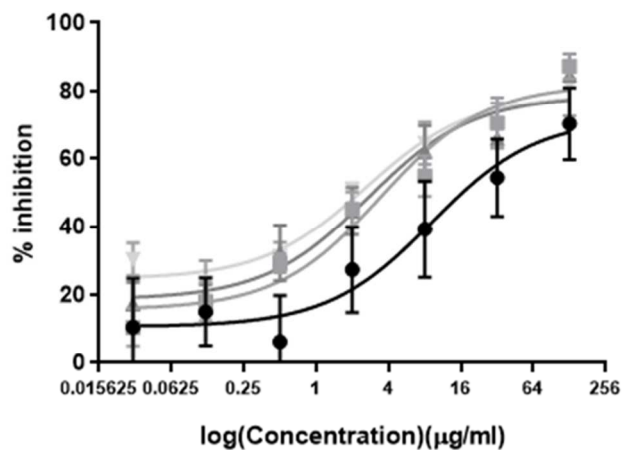
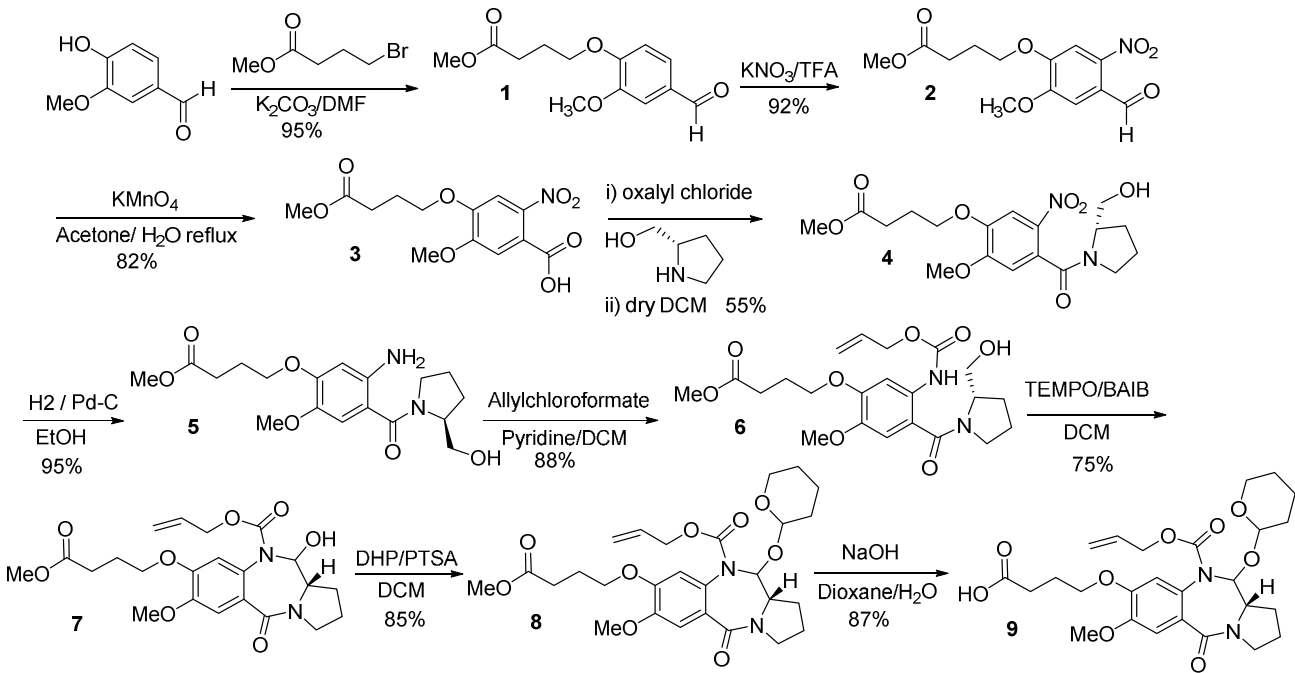
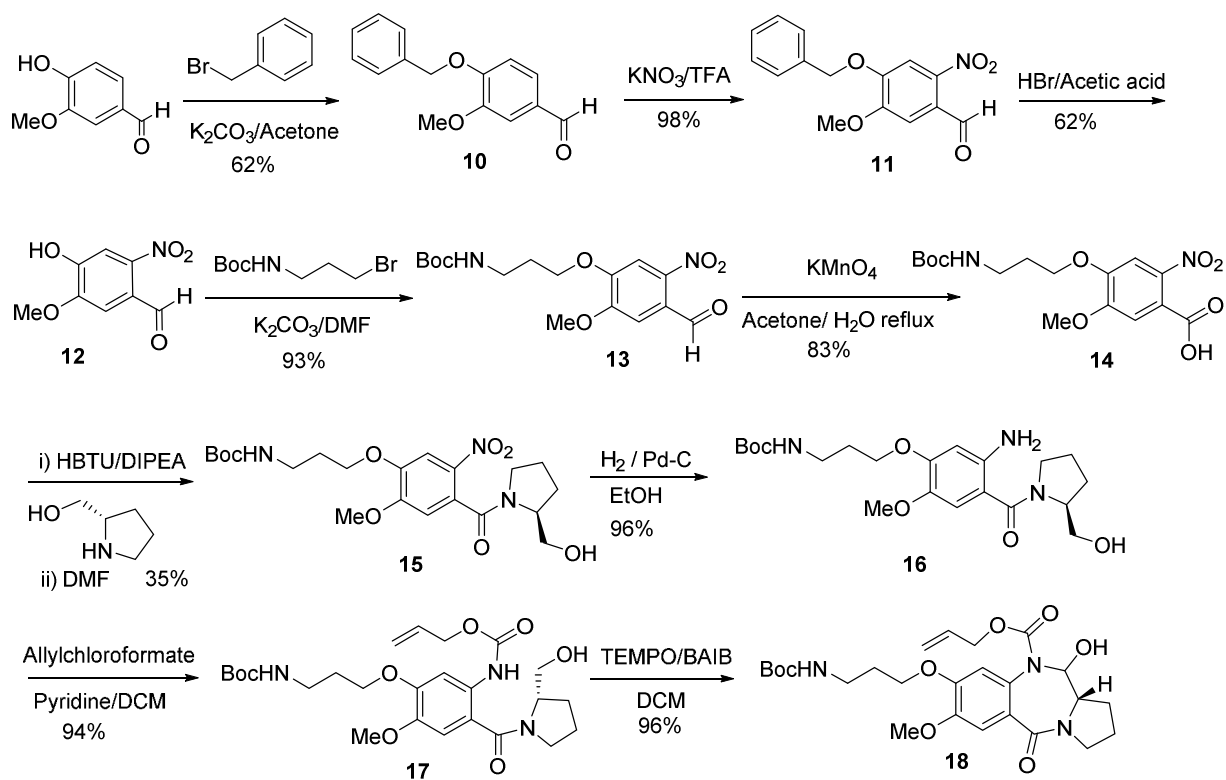


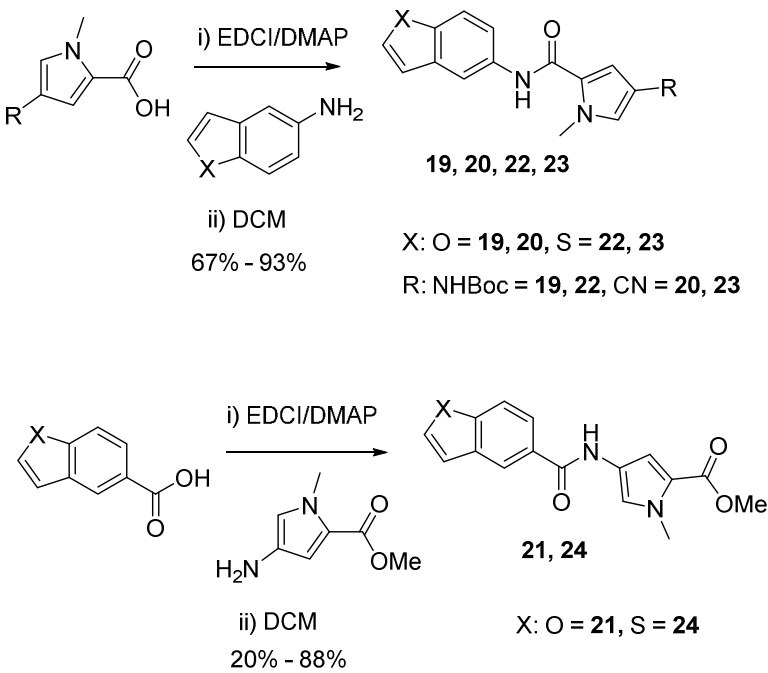
Figure 7. Biochemical analysis showing *S. aureus* gyrase enzyme inhibition by compounds **27** (■), **29** (▲), **30** (▼) and ciprofloxacin (●) which was used as a control.

SCHEMES

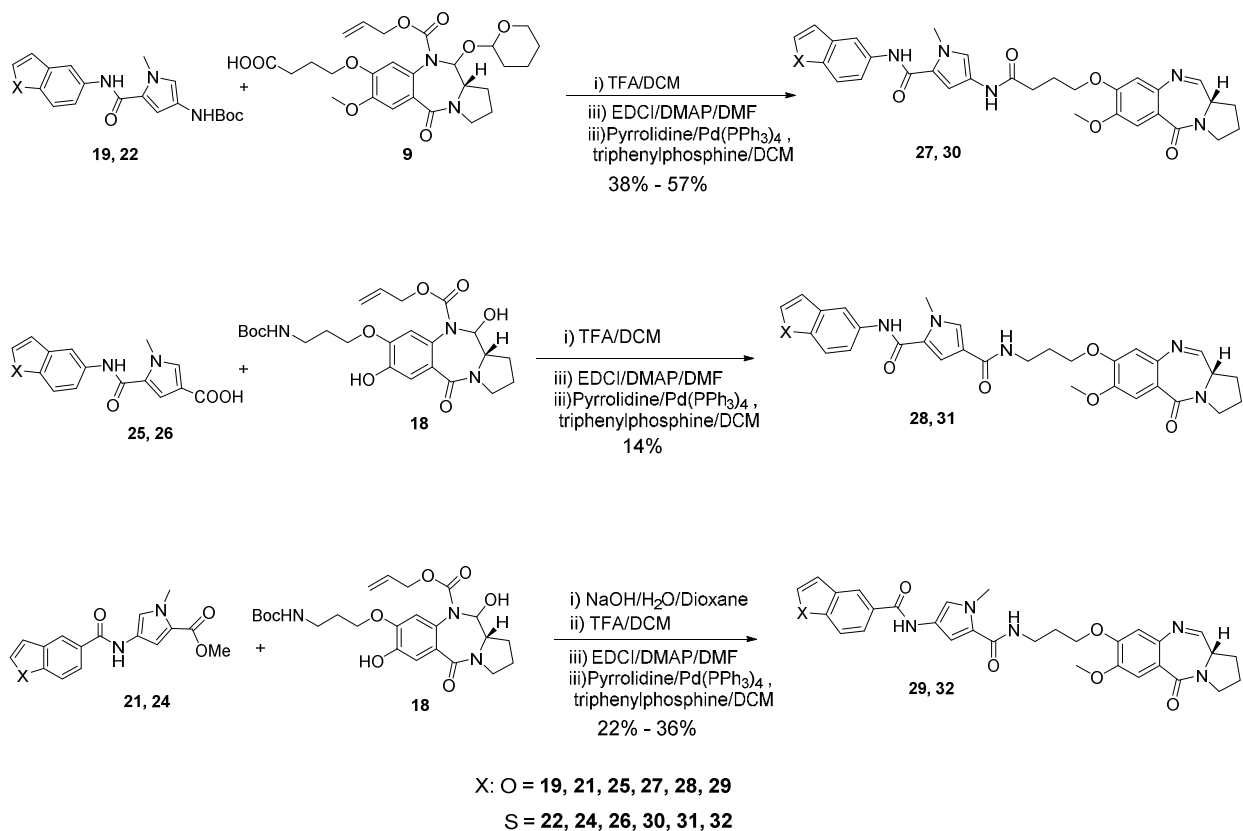


Scheme 1. Synthesis of PBD acid core 9

**Scheme 2.** Synthesis of PDB amino core **18**



31 **Scheme 3.** Generic amide coupling reactions in the synthesis of benzofused-*N*-methylpyrrole
32 intermediates
33
34
35
36
37
38
39
40
41
42
43
44
45
46
47
48
49
50
51
52
53
54
55
56
57
58
59
60



Scheme 4. Synthesis of standard and inverted orientation benzofused-*N*-methylpyrrole PBD derivatives.

TABLES

Table 1: DNA duplex stabilization for natural and inverted C8-PBD compounds. ΔT_m values are reported in the table in $^{\circ}\text{C}$ in comparison to the control. Assay conducted in triplicate.

Compounds	ΔT_m at 1 μM	
	Sequence	Sequence
	F1	F2
27	20.8 \pm 0.2	9.5 \pm 0.5
28	0.0 \pm 0.2	0.4 \pm 0.1
29	0.1 \pm 0.1	0.5 \pm 0.3
30	21.7 \pm 0.2	11.1 \pm 0.9
31	0.2 \pm 0.1	0.5 \pm 0.1
32	0.4 \pm 0.1	0.9 \pm 0.1
Netropsin	13.8 \pm 0.3	11.0 \pm 0.2
Ciprofloxacin	0.0 \pm 0.4	0.2 \pm 0.3

Table 2. Minimum inhibitory concentrations of C8-PBD benzofused analogues with natural and inverted building blocks against Gram-positive strains

Compound	Gram-positive strains MIC($\mu\text{g/mL}$)						IC ₅₀ ($\mu\text{g/mL}$)	
	VRE		VSE	MRSA		MSSA	WI38 HeLa	
	NCTC 12201	NCTC 12204	NCTC 775	EMRS A 15	EMRSA 16	ATCC 9144		
27	≤ 0.125	≤ 0.125	≤ 0.125	≤ 0.125	≤ 0.125	≤ 0.125	0.14	0.03
28	2	2	16	>32	>32	16	>28.4	>28.4
29	0.5	1	4	2	4	2	>28.4	>28.4
30	≤ 0.125	≤ 0.125	≤ 0.125	≤ 0.125	≤ 0.125	≤ 0.125	0.07	0.03
31	2-4	≤ 0.125	1	>32	>32	16	>28.4	>28.4
32	≤ 0.125	≤ 0.125	≤ 0.125	>32	>32	16	>28.4	>28.4
Cipro	0.5	2	1	32	32	≤ 0.125	>28.4	>28.4

Table 3. Energy values calculated using Poisson Boltzmann model and Generalized Born model and expressed as kcal/mol for each DNA-compound complex

Complex	ΔG_{GB}	ΔG_{PB}
	(kcal/mol)	(kcal/mol)
Seq1-27	-39	-40
Seq1-28	-34	-35
Seq1-29	-33	-35
Seq1-30	-42	-43
Seq1-31	-36	-39
Seq1-32	-35	-38
Seq2-27	-38	-39
Seq2-28	-37	-38
Seq2-29	-36	-37
Seq2-30	-42	-43
Seq2-31	-38	-40
Seq2-32	-37	-40
Seq3-27	-41	-43
Seq3-28	-38	-39
Seq3-29	-37	-39
Seq3-30	-43	-45
Seq3-31	-37	-39
Seq3-32	-38	-39

ASSOCIATED CONTENT

Supporting information.

Supporting information is available containing:

Dynamic Light Scattering, *In silico* screening method, LC-Ms method, NMR spectra and HRMS
Molecular formula strings (CSV)

ORCID

Khondaker M. Rahman: 0000-0001-8566-8648

Notes

The authors declare no competing financial interest.

ACKNOWLEDGMENT

We gratefully acknowledge the support provided by the High- Performance Compute Cluster (HPC) of King's College London (Ada) and to Dr Stuart Jones for his help with Dynamic Light Scattering experiment. We are thankful to Erasmus+ research funding scheme for providing a scholarship to PA and Public Health England for supporting this work (Award code JGALAQR, JGALAVR).

ABBREVIATIONS

PBD, pyrrolbenzodiazepine, MDR, multi-drug resistant; HTS, high-throughput screening; MRSA, methicillin resistant *S. aureus*; VRE, vancomycin resistant *Enterococci*; HBTU, 2-(1H-benzotriazol-1-yl)-1,1,3,3-tetramethyluronium hexafluorophosphate; DIPEA, N,N-diisopropylethylamine; FRET, fluorescence resonance energy transfer; FAM, 6-Carboxyfluorescein; TAMRA, 5-Carboxytetramethylrhodamine., m.p., Melting Point

REFERENCE

[1] Ventola, C. L. (2015) The antibiotic resistance crisis: part 1: causes and threats, *Phar. Ther.* 40, 277.

[2] Laxminarayan, R., Duse, A., Wattal, C., Zaidi, A. K., Wertheim, H. F., Sumpradit, N., Vlieghe, E., Hara, G. L., Gould, I. M., and Goossens, H. (2013) Antibiotic resistance—the need for global solutions, *Lancet Infect. Dis.* 13, 1057-1098, doi: 10.1016/S1473-3099(13)70318-9

[3] Rice, L. B. (2008) Federal funding for the study of antimicrobial resistance in nosocomial pathogens: no ESKAPE, *J. Infect. Dis.* 197, 1079 –1081, doi: 10.1086/533452

[4] McGowan Jr, J. E. (2001) Economic impact of antimicrobial resistance, *Emerging Infect. Dis.* 7, 286-292, doi: 10.3201/eid0702.700286

[5] Giske, C. G., Monnet, D. L., Cars, O., and Carmeli, Y. (2008) Clinical and economic impact of common multidrug-resistant gram-negative bacilli, *Antimicrob. Agents Ch.* 52, 813-821, doi: 10.1128/AAC.01169-07

[6] Cosgrove, S. E., and Carmeli, Y. (2003) The impact of antimicrobial resistance on health and economic outcomes, *Clin. Infect. Dis.* 36, 1433-1437, doi: 10.1086/375081/304950

[7] Roca, I., Akova, M., Baquero, F., Carlet, J., Cavaleri, M., Coenen, S., Cohen, J., Findlay, D., Gyssens, I., and Heure, O. (2015) The global threat of antimicrobial resistance: science for intervention, *New Microb. New Infect.* 6, 22-29, doi: 10.1016/j.nmni.2015.02.007

[8] Silver, L. L. (2011) Challenges of antibacterial discovery, *Clin. Microbiol. Rev.* 24, 71-109, doi: 10.1128/CMR.00030-10

[9] Boucher, H. W., Talbot, G. H., Bradley, J. S., Edwards, J. E., Gilbert, D., Rice, L. B., Scheld, M., Spellberg, B., and Bartlett, J. (2009) Bad bugs, no drugs: no ESKAPE! An update from the Infectious Diseases Society of America, *Clin. Infect. Dis.* 48, 1-12, doi: 10.1086/595011

[10] Fischbach, M. A., and Walsh, C. T. (2009) Antibiotics for emerging pathogens, *Science* 325, 1089-1093, doi: 0.1126/science.1176667

[11] Antonow, D., and Thurston, D. E. (2011) Synthesis of DNA-interactive pyrrolo[2,1-c][1,4]benzodiazepines (PBDs), *Chem. Rev.* 111, 2815-2864, doi: 10.1021/cr100120f

[12] Gerratana, B. (2012) Biosynthesis, synthesis, and biological activities of pyrrolobenzodiazepines, *Med. Res. Rev* 32, 254-293, doi: 10.1002/med.20212

- [13] Mantaj, J., Jackson, P. J. M., Rahman, K. M., and Thurston, D. E. (2017) From Anthramycin to Pyrrolobenzodiazepine (PBD)-Containing Antibody–Drug Conjugates (ADCs), *Angew. Chem. Int. Edit.* *56*, 462-488, doi: 10.1002/anie.201510610
- [14] Rahman, K. M., James, C. H., Bui, T. T., Drake, A. F., and Thurston, D. E. (2011) Observation of a single-stranded DNA/pyrrolobenzodiazepine adduct, *J. Am. Chem. Soc.* *133*, 19376-19385, doi: 10.1021/ja205395r
- [15] Thurston, D. E., Bose, D. S., Thompson, A. S., Howard, P. W., Leoni, A., Croker, S. J., Jenkins, T. C., Neidle, S., Hartley, J. A., and Hurley, L. H. (1996) Synthesis of sequence-selective C8-linked pyrrolo [2, 1-c][1, 4] benzodiazepine DNA interstrand cross-linking agents, *J Org. Chem.* *61*, 8141-8147, doi: 10.1021/jo951631s
- [16] Leimgruber, W., Stefanović, V., Schenker, F., Karr, A., and Berger, J. (1965) Isolation and characterization of anthramycin, a new antitumor antibiotic, *J. Am. Chem. Soc.* *87*, 5791-5793, doi: 10.1021/ja00952a050
- [17] Hertzberg, R. P., Hecht, S. M., Reynolds, V. L., Molineux, I. J., and Hurley, L. H. (1986) DNA-sequence specificity of the pyrrolo 1,4 benzodiazepine antitumor antibiotics - Methidiumpropyl-EDTA-iron(ii) footprinting analysis of DNA-binding sites for anthramycin and related drugs, *Biochemistry* *25*, 1249-1258, doi: 10.1021/bi00354a009
- [18] Hurley, L. H., Reck, T., Thurston, D. E., Langley, D. R., Holden, K. G., Hertzberg, R. P., Hoover, J. R. E., Gallagher, G., Faucette, L. F., Mong, S. M., and Johnson, R. K. (1988) Pyrrolo 1,4 benzodiazepine antitumor antibiotics - relationship of DNA alkylation and sequence specificity to the biological-activity of natural and synthetic compounds, *Chem. Res. Toxicol.* *1*, 258-268, doi: 10.1021/tx00005a002
- [19] Puvvada, M. S., Forrow, S. A., Hartley, J. A., Stephenson, P., Gibson, I., Jenkins, T. C., and Thurston, D. E. (1997) Inhibition of bacteriophage T7 RNA polymerase in vitro transcription by DNA-binding pyrrolo 2,1-c 1,4 benzodiazepines, *Biochemistry* *36*, 2478-2484, doi: 10.1021/bi952490r
- [20] Rahman, K. M., Vassoler, H., James, C. H., and Thurston, D. E. (2010) DNA Sequence Preference and Adduct Orientation of Pyrrolo[2,1-c][1,4]benzodiazepine Antitumor Agents, *ACS Med. Chem. Lett.* *1*, 427-432, doi: 10.1021/ml100131b
- [21] Hartley, J. A., Spanswick, V. J., Brooks, N., Clingen, P. H., McHugh, P. J., Hochhauser, D., Pedley, R. B., Kelland, L. R., Alley, M. C., and Schultz, R. (2004) SJG-136 (NSC

- 694501), a novel rationally designed DNA minor groove interstrand cross-linking agent with potent and broad spectrum antitumor activity, *Cancer Res.* **64**, 6693-6699, doi: 10.1158/0008-5472.CAN-03-2941
- [22] Rosado, H., Rahman, K. M., Feuerbaum, E.-A., Hinds, J., Thurston, D. E., and Taylor, P. W. (2011) The minor groove-binding agent ELB-21 forms multiple interstrand and intrastrand covalent cross-links with duplex DNA and displays potent bactericidal activity against methicillin-resistant *Staphylococcus aureus*, *J. Antimicrob. Chemoth.* **66**, 985-996, doi: 10.1093/jac/dkr044
- [23] Antonow, D., and Thurston, D. E. (2010) Synthesis of DNA-interactive pyrrolo [2, 1-c][1, 4] benzodiazepines (PBDs), *Chem. Rev.* **111**, 2815-2864, doi: 10.1021/cr100120f
- [24] Rahman, K. M., Rosado, H., Moreira, J. B., Feuerbaum, E.-A., Fox, K. R., Stecher, E., Howard, P. W., Gregson, S. J., James, C. H., de la Fuente, M., Waldron, D. E., Thurston, D. E., and Taylor, P. W. (2012) Antistaphylococcal activity of DNA-interactive pyrrolobenzodiazepine (PBD) dimers and PBD-biaryl conjugates, *J. Antimicrob. Chemoth.* **67**, 1683-1696, doi: 10.1093/jac/dks127
- [25] Rahman, K. M., Jackson, P. J., James, C. H., Basu, B. P., Hartley, J. A., de la Fuente, M., Schatzlein, A., Robson, M., Pedley, B., and Pepper, C. (2013) C8-linked pyrrolobenzodiazepine (PBD)-biaryl conjugates with femtomolar in vitro cytotoxicity and in vivo antitumour activity in mouse models of pancreatic and breast cancer, *Cancer Res.* **73**, 1129-1129, doi: 10.1021/jm301882a
- [26] Kotecha, M., Kluza, J., Wells, G., O'Hare, C. C., Forni, C., Mantovani, R., Howard, P. W., Morris, P., Thurston, D. E., and Hartley, J. A. (2008) Inhibition of DNA binding of the NF-Y transcription factor by the pyrrolobenzodiazepine-polyamide conjugate GWL-78, *Mol. Cancer Ther.* **7**, 1319-1328, doi: 10.1158/1535-7163.MCT-07-0475
- [27] Rahman, K. M., Jackson, P. J., James, C. H., Basu, B. P., Hartley, J. A., de la Fuente, M., Schatzlein, A., Robson, M., Pedley, R. B., and Pepper, C. (2013) GC-targeted C8-linked pyrrolobenzodiazepine-biaryl conjugates with femtomolar in vitro cytotoxicity and in vivo antitumor activity in mouse models, *J. Med. Chem.* **56**, 2911-2935, doi: 10.1021/jm301882a
- [28] Tiberghien, A. C., Evans, D. A., Kiakos, K., Martin, C. R., Hartley, J. A., Thurston, D. E., and Howard, P. W. (2008) An asymmetric C8/C8'-tripyrrole-linked sequence-selective

- pyrrolo [2, 1-c][1, 4] benzodiazepine (PBD) dimer DNA interstrand cross-linking agent spanning 11 DNA base pairs, *Bioorg. Med. Chem. Lett.* 18, 2073-2077, 10.1016/j.bmcl.2008.01.096
- [29] Renčiuk, D., Zhou, J., Beaupaire, L., Guédin, A., Bourdoncle, A., and Mergny, J.-L. (2012) A FRET-based screening assay for nucleic acid ligands, *Methods* 57, 122-128, doi: 10.1016/j.ymeth.2012.03.020
- [30] Gregson, S. J., Howard, P. W., Hartley, J. A., Brooks, N. A., Adams, L. J., Jenkins, T. C., Kelland, L. R., and Thurston, D. E. (2001) Design, synthesis, and evaluation of a novel pyrrolobenzodiazepine DNA-interactive agent with highly efficient cross-linking ability and potent cytotoxicity, *J. Med. Chem.* 44, 737-748, doi: 10.1021/jm001064n
- [31] Mosmann, T. (1983) Rapid colorimetric assay for cellular growth and survival: application to proliferation and cytotoxicity assays, *J Immunol. Methods* 65, 55-63, doi: 10.1016/0022-1759(83)90303-4
- [32] Kamal, A., Ramesh, G., Laxman, N., Ramulu, P., Srinivas, O., Neelima, K., Kondapi, A. K., Sreenu, V., and Nagarajaram, H. (2002) Design, synthesis, and evaluation of new noncross-linking pyrrolobenzodiazepine dimers with efficient DNA binding ability and potent antitumor activity, *J. Med.Chem.* 45, 4679-4688, doi: 10.1021/jm020124h
- [33] Miles, A. A., Misra, S., and Irwin, J. (1938) The estimation of the bactericidal power of the blood, *Epidemiol. Infect.* 38, 732-749, doi: 10.1017/S002217240001158X
- [34] Maxwell, A., Burton, N. P., and O'Hagan, N. (2006) High-throughput assays for DNA gyrase and other topoisomerases, *Nucleic Acids Res* 34, e104, doi: 10.1093/nar/gkl504
- [35] Picconi, P., Hind, C., Jamshidi, S., Nahar, K., Clifford, M., Wand, M. E., Sutton, J. M., and Rahman, K. M. (2017) Triaryl Benzimidazoles as a New Class of Antibacterial Agents against Resistant Pathogenic Microorganisms, *J Med. Chem.* 60, 6045-6059, doi: 10.1021/acs.jmedchem.7b00108
- [36] Koes, D. R., Baumgartner, M. P., and Camacho, C. J. (2013) Lessons learned in empirical scoring with smina from the CSAR 2011 benchmarking exercise, *J. Chem. inf Model.* 53, 1893-1904, doi: 10.1021/ci300604z
- [37] Darden, T. Y., D.; Pedersen, L. . (1993) Particle Mesh Ewald - an N.Log(N) Method for Ewald Sums in Large Systems, *J. Chem. Phys.* 98, 10089-10093, doi: 10.1063/1.464397

- [38] Ryckaert, J. P. C., G.; Berendsen, H. J. C. (1977) Numerical-Integration of Cartesian Equations of Motion of a System with Constraints - Molecular-Dynamics of N-Alkanes, *J. Comput. Phys.* **23**, 327-341, doi: 10.1016/0021-9991(77)90098-5
- [39] Case, D. A., Cheatham, T. E., Darden, T., Gohlke, H., Luo, R., Merz, K. M., Onufriev, A., Simmerling, C., Wang, B., and Woods, R. J. (2005) The Amber biomolecular simulation programs, *J. Comput. Chem.* **26** 1668-1688.
- [40] Case, D. A., Darden, T. A., Cheatham, T. E., Simmerling, C. L., Wang, J., Duke, R. E., Luo, R., Walker, R. C., Zhang, W., Merz, K. M., Roberts, B., Hayik, S., Roitberg, A., Seabra, G., Swails, J., Götz, A. W., Kolossváry, I., Wong, K. F., Paesani, F., Vanicek, J., Wolf, R. M., Liu, J., Wu, X., Brozell, S. R., Steinbrecher, T., Gohlke, H., Cai, Q., Wang, X., Ye, J., Hsieh, M.-J., Cui, G., Roe, D. R., Mathews, D. H., Seetin, M. G., Salomon-Ferrer, R., Sagui, C., Babin, V., Luchko, T., Gusarov, S., Kovalenko, A., and Kollman, P. A. (2012) AMBER 12, *University of California, San Francisco*.
- [41] Wang, W., and Kollman, P. A. (2000) Free energy calculations on dimer stability of the HIV protease using molecular dynamics and a continuum solvent model, *J. Mol. Biol.* **303**, 567-582. doi: 10.1006/jmbi.2000.4057
- [42] Weiser, J., Shenkin, P. S., and Still, W. C. (1999) Approximate atomic surfaces from linear combinations of pairwise overlaps (LCPO), *J. Comput. Chem.* **20**, 217-230, doi: 10.1002/(SICI)1096-987X(19990130)20:2<217::AID-JCC4>3.0.CO;2-A

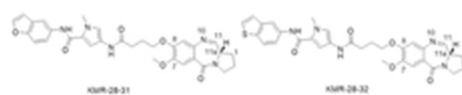


Figure 1. Structure of KMR-28 31 (27, PBD-Py-Bzf) and KMR-28 32 (30, PBD-Py-Bzt), previously reported C8-benzofused PBDs with antistaphylococcal activity ($\text{MIC} \leq 0.125 \mu\text{g/mL}$).

20x4mm (300 x 300 DPI)

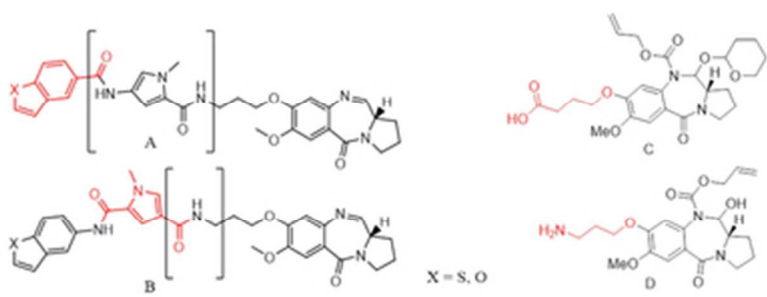


Figure 2. A) &B), Structures showing (in brackets) the reverse moieties and (in red) the different building blocks from the reference compounds; C) Traditional PBD core with 4C-acid linker; D) New PBD core with 4C-amine linker.

35x14mm (300 x 300 DPI)

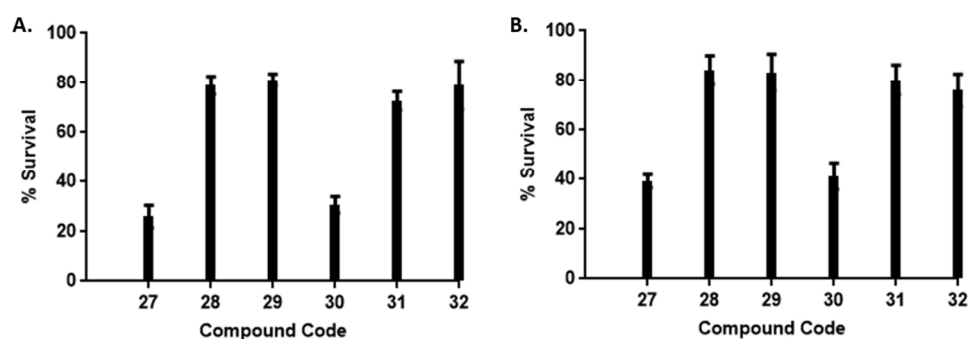


Figure 3. Eukaryotic toxicity of the C8-Benzofused PBDs with natural and inverted building blocks at 25 μ M after 24 h incubation against A) cervical cancer cell line HeLa and B) non-tumour lung fibroblast WI38.

160x57mm (300 x 300 DPI)

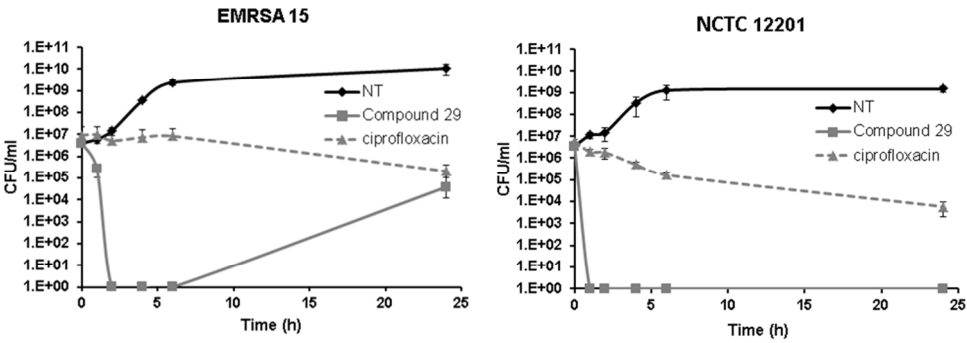


Figure 4. Response of EMRSA-15 and VRE-12201 strains to treatment with suprainhibitory concentrations (4 × MIC) of compound 29.

160x59mm (300 x 300 DPI)

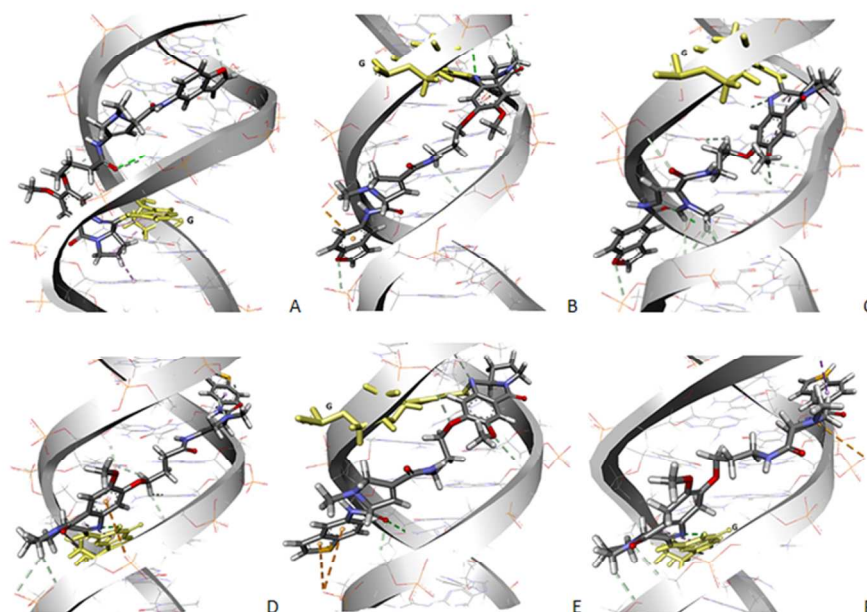


Figure 5. The covalent interactions between a random sequence of DNA and compound 27 (A), 28 (B), 29 (C) in the top panel and with 30 (D), 31 (E) and 32(F) in lower panel. All compounds lay along the minor groove of DNA and form covalent interaction to the exocyclic N2 atom of NH₂ group of a Guanine (in yellow sticks) with their C11 atom present in C=N imine bond.

160x113mm (300 x 300 DPI)

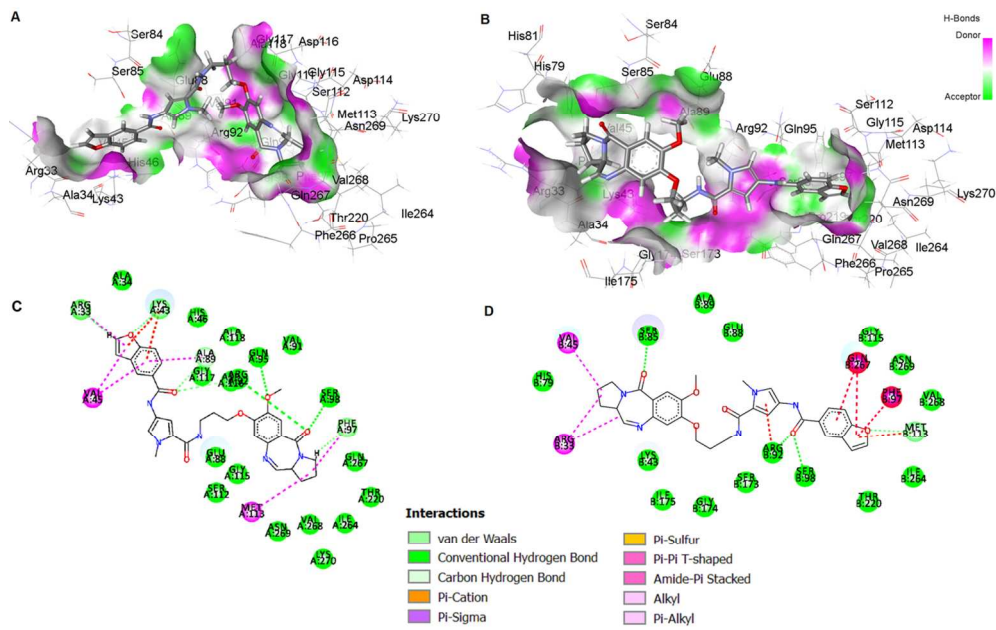


Figure 6. A) Molecular model showing the interaction of compound 29 with the subunit-1 of the *S. aureus* gyrase A; B) Molecular model showing the interaction of compound 29 with the subunit-2 of the *S. aureus* gyrase A; C) 2D model showing the Key interactions between compound 29 with the binding site in the subunit-1 of the *S. aureus* gyrase A; D) 2D model showing the key interactions between compound 29 with the binding site in the subunit-2 of the *S. aureus* gyrase A.

160x102mm (300 x 300 DPI)

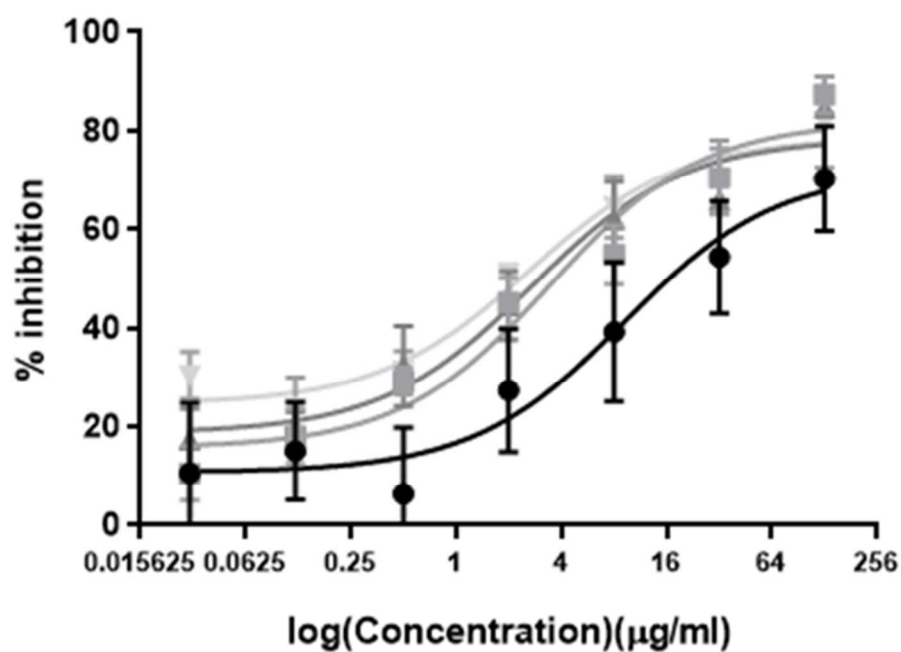


Figure 7. Biochemical analysis showing *S. aureus* gyrase enzyme inhibition by compounds 27 (■), 29 (▲), 30 (▼) and ciprofloxacin (●) which was used as a control.

82x59mm (300 x 300 DPI)

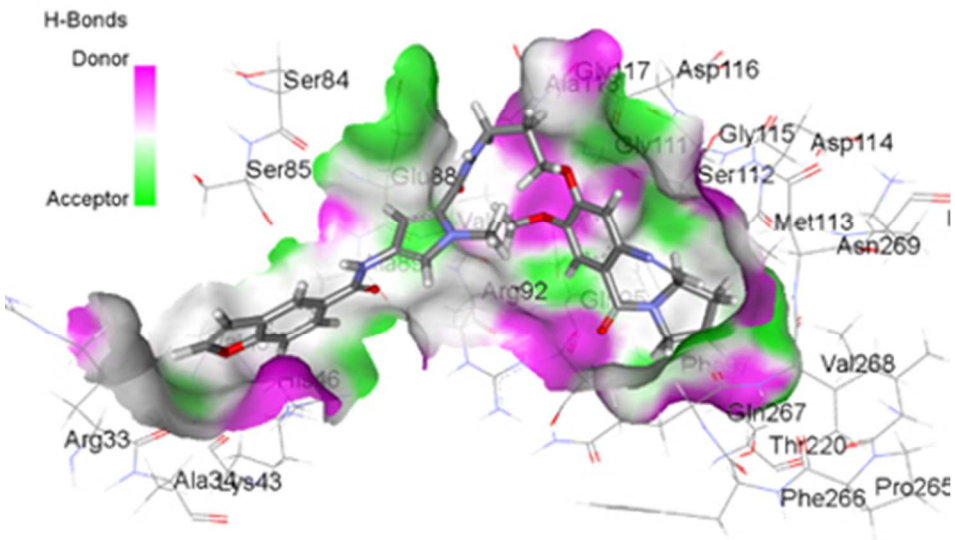


Table of Content Graphic

39x23mm (300 x 300 DPI)